

AD-750 867

A STUDY OF THE JET STRETCHER CONCEPT FOR  
ANGLE-OF-ATTACK TESTING

R. C. Bauer, et al

Arnold Engineering Development Center  
Arnold Air Force Station, Tennessee

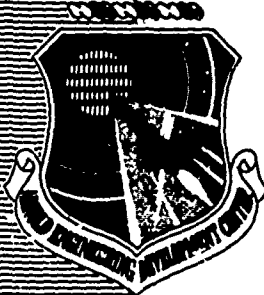
October 1972

DISTRIBUTED BY:

**NTIS**

National Technical Information Service  
U. S. DEPARTMENT OF COMMERCE  
5285 Port Royal Road, Springfield Va. 22151

AEDC-TR-72-150

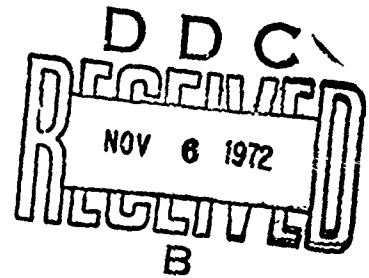


AD 750867

**A STUDY OF THE JET STRETCHER  
CONCEPT FOR ANGLE-OF-ATTACK TESTING**

**R. C. Bauer, R. L. Barebo, and E. H. Matkins  
ARO, Inc.**

October 1972



Approved for public release; distribution unlimited.

Reprinted by  
NATIONAL TECHNICAL  
INFORMATION SERVICE  
U.S. Department of Commerce  
Springfield, MA 01115

**ENGINE TEST FACILITY  
ARNOLD ENGINEERING DEVELOPMENT CENTER  
AIR FORCE SYSTEMS COMMAND  
ARNOLD AIR FORCE STATION, TENNESSEE**

45  
R

# NOTICES

When U. S. Government drawings specifications, or other data are used for any purpose other than a definitely related Government procurement operation, the Government thereby incurs no responsibility nor any obligation whatsoever, and the fact that the Government may have formulated, furnished, or in any way supplied the said drawings, specifications, or other data, is not to be regarded by implication or otherwise, or in any manner licensing the holder or any other person or corporation, or conveying any rights or permission to manufacture, use, or sell any patented invention that may in any way be related thereto.

Qualified users may obtain copies of this report from the Defense Documentation Center.

References to named commercial products in this report are not to be considered in any sense as an endorsement of the product by the United States Air Force or the Government.

ADDITIONAL TO	
NTIS	White Section <input checked="" type="checkbox"/>
O & C	Def. Section <input type="checkbox"/>
UNCLASSIFIED	<input type="checkbox"/>
.....	
.....	
By	
DISTRIBUTION AVAILABILITY CODES	
Dist. A MIL. & /or SP. CIAL.	
A	

UNCLASSIFIED

Security Classification

DOCUMENT CONTROL DATA - R & D

(Security classification of title, body of abstract and indexing annotation must be entered when the overall report is classified)

1. ORIGINATING ACTIVITY (Corporate author) Arnold Engineering Development Center Arnold Air Force Station, Tennessee 37389		2a. REPORT SECURITY CLASSIFICATION UNCLASSIFIED	
		2b. GROUP N/A	
3. REPORT TITLE A STUDY OF THE JET STRETCHER CONCEPT FOR ANGLE-OF-ATTACK TESTING			
4. DESCRIPTIVE NOTES (Type of report and inclusive dates) July 1, 1970, to June 30, 1971--Final Report			
5. AUTHOR(S) (First name, middle initial, last name) R. C. Bauer, R. L. Barebo, and E. H. Matkins, ARO, Inc.			
6. REPORT DATE October 1972		7a. TOTAL NO. OF PAGES 42	7b. NO. OF REFS 6
8a. CONTRACT OR GRANT NO.		9a. ORIGINATOR'S REPORT NUMBER(S) AEDC-TR-72-150	
b. PROJECT NO. 3012		9b. OTHER REPORT NO(S) (Any other numbers that may be assigned this report) ARO-ETF-TR-72-103	
c. Program Element 62402F			
d. Task 07			
10. DISTRIBUTION STATEMENT Approved for public release; distribution unlimited.			
11. SUPPLEMENTARY NOTES Available in DDC		12. SPONSORING MILITARY ACTIVITY Arnold Engineering Development Center, Arnold Air Force Station, Tennessee 37389	
13. ABSTRACT The feasibility of using a porous, axisymmetric jet stretcher for angle-of-attack testing of missiles having aft-located engine inlets was demonstrated. Initially, an analytical technique was developed for evaluating the performance of a jet stretcher and was applied to a small-scale experimental jet stretcher system for test body angles of attack of 4 and 8 deg. For each test body angle of attack, the analytical technique was used to determine the optimum position of the jet stretcher and the regions on the jet stretcher that require porosity. The experimental results verified the analytical technique and showed that it is possible to obtain good aerodynamic simulation for angles of attack up to 4.75 deg using an axisymmetric jet stretcher. The results also suggest a simple jet stretcher modification that will significantly increase the angle-of-attack capability of this testing technique.			

UNCLASSIFIED

Security Classification

14. KEY WORDS	LINK A		LINK B		LINK C	
	ROLE	WT	ROLE	WT	ROLE	WT
jet stretcher angle of attack analysis porosity aerodynamic simulation experimental data testing facilities						

APFC  
Form 478 Rev 7-66

I 3

UNCLASSIFIED

Security Classification

**A STUDY OF THE JET STRETCHER  
CONCEPT FOR ANGLE-OF-ATTACK TESTING**

**R. C. Bauer, R. L. Barebo, and E. H. Matkins  
ARO, Inc.**

Approved for public release; distribution unlimited.

10

## FOREWORD

The work reported herein was sponsored by the Arnold Engineering Development Center (AEDC), Air Force Systems Command (AFSC), Arnold Air Force Station, Tennessee, under Program Element 62402F, Project 3012, Task 07.

The results of the research presented herein were obtained by ARO, Inc., (a subsidiary of Sverdrup and Parcel and Associates, Inc.), contract operator of AEDC, AFSC, under Contract F40600-73-0004. The work was conducted in the Engine Test Facility (ETF) from July 1, 1970, to June 30, 1971, under ARO project No. RH5102 (RW5102). The manuscript for this report was submitted for publication on July 6, 1972.

The authors wish to acknowledge the assistance of W. C. Armstrong, CCO, who programmed the analysis.

This technical report has been reviewed and is approved.

MARION L. LASTER  
Research and Development  
Division  
Directorate of Technology

ROBERT O. DIETZ  
Acting Director  
Directorate of Technology

**ABSTRACT**

The feasibility of using a porous, axisymmetric jet stretcher for angle-of-attack testing of missiles having aft-located engine inlets was demonstrated. Initially, an analytical technique was developed for evaluating the performance of a jet stretcher and was applied to a small-scale experimental jet stretcher system for test body angles of attack of 4 and 8 deg. For each test body angle of attack, the analytical technique was used to determine the optimum position of the jet stretcher and the regions on the jet stretcher that require porosity. The experimental results verified the analytical technique and showed that it is possible to obtain good aerodynamic simulation for angles of attack up to 4.75 deg using an axisymmetric jet stretcher. The results also suggest a simple jet stretcher modification that will significantly increase the angle-of-attack capability of this testing technique.

## CONTENTS

	<u>Page</u>
ABSTRACT . . . . .	iii
NOMENCLATURE . . . . .	vi
I. INTRODUCTION . . . . .	1
II. ANALYSIS . . . . .	2
III. EXPERIMENTAL VERIFICATION . . . . .	3
IV. CONCLUSIONS . . . . .	8
REFERENCES . . . . .	9

## APPENDIXES

## I. ILLUSTRATIONS

Figure

1. Jet Stretcher Arrangement with Test Vehicle at Zero Angle of Attack . . . . .	13
2. Sketch Showing Jet Stretcher Mismatch Angle $\beta$ . . . . .	14
3. Experimental Jet Stretcher-Diffuser System . . . . .	15
4. Jet Stretcher Mismatch Angle for Design Configuration . . . . .	16
5. Test Configuration with Test Body and Jet Stretcher at Zero Angle of Attack . . . . .	17
6. Test Body Pressure Distribution for Zero Angle of Attack . . . . .	18
7. Test Configuration with Test Body at 4-deg and Jet Stretcher at 1.5-deg Angles of Attack . . . . .	19
8. Jet Stretcher Mismatch Angle with Test Body at 4-deg and Jet Stretcher at 1.5-deg Angles of Attack . . . . .	20
9. Jet Stretcher Porosity . . . . .	21
10. Test Body Pressure Distribution for 4-deg Angle of Attack . . . . .	22
11. Test Configuration with Test Body at 8-deg and Jet Stretcher at 3.5-deg Angles of Attack . . . . .	27
12. Jet Stretcher Mismatch Angle with Test Body at 8-deg and Jet Stretcher at 3.5-deg Angles of Attack . . . . .	28
13. Test Body Pressure Distribution for 8-deg Angle of Attack . . . . .	29
14. Application of Jet Stretcher with Spacers . . . . .	34
II. TABLE	
I. Measured Jet Stretcher Coordinates . . . . .	35
II. APPROXIMATE MACH LINE ANALYSIS . . . . .	36

Preceding page blank

### NOMENCLATURE

$C_p$	Pressure coefficient, $(p_B - P_N)/q_N$
$M$	Mach number
$m$	Ordinate of approximate Mach line center (Fig. III-1)
$n$	Station of approximate Mach line center (Fig. III-1)
$p$	Static pressure, psia
$p_t$	Total pressure, psia
$q$	Dynamic pressure, psia
$R$	Radius, in.
$r$	Radius of approximate Mach line (Fig. III-1), in.
$T_t$	Total temperature, °R
$X$	Station along centerline, in.
$\alpha$	Angle relative to nozzle centerline, deg
$\beta$	Mismatch angle between jet stretcher surface and the interference-free flow field, deg
$\gamma$	Ratio of specific heats
$\delta$	Total boundary layer thickness, in.
$\epsilon$	Flow angle relative to test body centerline, deg
$\epsilon_j$	Jet stretcher surface angle relative to jet stretcher centerline, deg
$\theta$	Radial angle measured from leeward side of test body, deg
$\mu$	Mach angle, deg

### SUBSCRIPTS

$B$	Test body
$B_i$	Originating point of approximate Mach line
$B_t$	Terminating point of approximate Mach line

- BS Test body surface
- c Jet stretcher ambient
- j Jet stretcher
- N Nozzle

## SECTION I INTRODUCTION

The simulation of supersonic flow conditions surrounding a body of revolution in a ground test facility has been a source of study and experimentation ever since the advent of supersonic aerodynamics. Accurate flow simulation requires that no influences from the surrounding test cell occur which would disturb the flow conditions surrounding the test model. This becomes of increasing importance when the flow conditions on the aft portion of the model must be simulated, as in the case of an airbreathing propulsion system operating at low altitude, with the vehicle inlets mounted on the rear portion of the test vehicle. The requirement for testing the inlet and engine as a complete system is necessary in many missile and air-frame configurations because of the strong aerodynamic coupling between the forebody and inlets which influence the overall engine performance. At zero angle of attack, it is possible through proper nozzle design to simulate the flow approaching an aft-mounted inlet by letting the test vehicle forebody become the centerbody of the test nozzle, or it may be possible to test the inlet-engine system without the forebody by designing the approaching air passages to simulate the inlet flow. Unfortunately, neither of these approaches is adequate for meeting the requirement for testing multiple inlet configurations at finite angles of attack.

There are three methods that can be utilized for simulating the flow approaching an aft-mounted engine inlet on a full-scale test vehicle at angle of attack. First, a large supersonic wind tunnel with porous walls for shock cancellation and boundary layer control, similar to the Arnold Engineering Development Center (AEDC) Propulsion Wind Tunnel (16S), could be used. However, in this facility the lower test altitude is limited to 55,000 and 80,000 ft at corresponding Mach numbers of 2.0 and 3.0. Second, a large free-jet nozzle with a solid-wall test section could be used which would allow any expansion waves from the nozzle or shock waves reflected from the test cell walls to intersect the test vehicle downstream of the engine inlet. Unfortunately, this method is usually limited by the mass flow requirements which exceed current facility capabilities. The third method employs a cowling-like structure, called a jet stretcher (Fig. 1, Appendix I), which stretches (or extends) the supersonic flow field produced by a relatively small nozzle. This type of facility requires mass flows as much as an order of magnitude smaller than the first two methods and will, therefore, permit the testing of full-scale low-altitude, high Mach number, airbreathing propulsion systems with aft-mounted inlets using the capabilities of existing facilities.

The jet stretcher (or jet extender, as it has been called by some) is basically an aerodynamically tailored device which replaces a known streamline or stream surface in the flow about the test vehicle with a boundary layer corrected wall, or shroud, and provides an interference-free flow field entering the inlets. To accomplish this, the jet stretcher must be positioned aft of the bow shock generated by the forebody nose and forward of any expansion or compression waves generated at the nozzle exit to prevent external disturbances from influencing the pressure on the test model and in the surrounding flow field.

Previous jet stretcher studies (such as Ref. 1) were primarily concerned with verification of the jet stretcher concept for zero angle-of-attack testing. In this report, the feasibility of the jet stretcher concept for finite angle-of-attack testing is investigated.

## SECTION II ANALYSIS

The testing of an axisymmetric vehicle at zero angle of attack requires an axisymmetric jet stretcher. To test this same vehicle at a finite angle of attack requires a jet stretcher having an unsymmetrical, three-dimensional, internal surface. Since the fabrication of such a surface is impractical at the present time, only axisymmetric or simply modified axisymmetric jet stretchers are of practical interest. The possibility of using an axisymmetric jet stretcher for angle-of-attack testing is indicated by the experimental results presented in Ref. 1. These results show that, for a finite angle of attack of the test vehicle with the jet stretcher at zero angle of attack, major disturbances originate from the top (leeward side of test vehicle) and bottom (windward side of test vehicle) regions of the jet stretcher, whereas the sides remain acceptably matched to the interference-free flow field. In addition, these disturbances result from opposite processes, i.e., expansion from the top and compression from the bottom, thus indicating that the disturbances can be reduced or eliminated by simply pitching the jet stretcher to an angle of attack. Intuitively, the remaining disturbances, if any, could be further reduced by bleed flow through selected porous regions on the jet stretcher surface. This combination of pitching the jet stretcher and the use of bleed flow is the approach followed in this study.

To use a jet stretcher, designed for a test body at zero angle of attack and a given Mach number, at finite angle of attack (off design condition) requires the establishment of a criterion for acceptable jet stretcher performance that is consistent with the test objectives. To test the engine in a vehicle similar to that shown in Fig. 1 requires a simulation of the forebody aerodynamics sufficient to allow the natural development and possible separation of the forebody boundary layer, either of which influence the flow at the inlets of the air induction system. Some experimental results indicate that acceptable aerodynamic simulation is achieved when the static pressure distribution on the test body is within  $\pm 10$  percent of that produced by an interference-free flow field. This criterion is used in this study since it is probably adequate for most engine test programs. However, an acceptable criterion for jet stretcher performance should be based on the objectives of each specific test program.

For the test body static pressure distribution to be within  $\pm 10$  percent, the jet stretcher static pressure distribution must be within  $\pm 5$  percent since a disturbance produced by the jet stretcher approximately doubles in magnitude when it strikes the test body. Therefore, the maximum acceptable angular misalignment between the jet stretcher and the interference-free flow field (expressed as  $\beta$  in Fig. 2) can be estimated from the following equations for small disturbances:

$$\beta_{\max} = \pm(0.05/\gamma M^2)\sqrt{M^2-1} \quad (\text{radians}) \quad (1)$$

Based on this equation, the maximum allowable angular misalignment of the jet stretcher varies from  $\pm 0.886$  to  $\pm 0.56$  deg in the Mach number range from 2.0 to 3.5. Since this is a highly simplified analysis, a conservative value of  $\pm 0.5$  deg was used.

To summarize then, an axisymmetric jet stretcher designed for a fixed Mach number and zero angle of attack can be used for various other Mach numbers and finite angles of attack by locating the jet stretcher such that the local mismatch in angle ( $\beta$ , Fig. 2) between the interference-free flow field and the jet stretcher surface is within a prescribed tolerance. If this is not possible over the entire jet stretcher surface (that can influence the flow field of interest), then only the jet stretcher inlet is matched within the prescribed tolerance. The remaining portions of the jet stretcher that exceed the prescribed tolerance can be corrected by making these surfaces porous and using bleed flow to reduce the disturbances.

The jet stretcher matching calculation for a finite test body angle of attack is greatly simplified by the previously mentioned experimental result that major disturbances originate from the top and bottom regions of jet stretcher while the sides remain acceptably matched to the interference-free flow field. Therefore, if it is possible to acceptably match the top and bottom of the jet stretcher, then it is reasonable to assume that the entire jet stretcher surface is acceptably matched to the interference-free flow field.

### SECTION III EXPERIMENTAL VERIFICATION

#### 3.1 OBJECTIVE

Experiments were conducted to verify the analytical technique for positioning the zero angle-of-attack jet stretcher for test body angles of attack of 4 and 8 deg.

#### 3.2 EXPERIMENTAL APPARATUS

##### 3.2.1 Description

A sketch of the experimental apparatus is presented in Fig. 3. This is the same apparatus used in the study reported in Ref. 1 except that the jet stretcher inlet was machined back 0.16 in. to eliminate a fabrication error. The apparatus consisted of a nominal 8-in exit-diam, Mach number 3.00 nozzle; a 3.5-in-diam test body with a 292 von Kármán forebody; and an axisymmetric jet stretcher. The test body was sting supported and could be rolled to obtain radial pressure distribution. The nozzle and jet stretcher were corrected for boundary layer based on a nozzle inlet total pressure of 30 psia and a total temperature of  $560^{\circ}\text{R}$ . The measured coordinates of the jet stretcher are presented in Table I (Appendix II).

### 3.2.2 Instrumentation

The parameters measured were the following:

1. Nozzle total pressure,  $p_{tN}$
2. Nozzle total temperature,  $T_{tN}$
3. Nozzle exit static pressure,  $p_N$  (tap located 0.62 in. upstream of nozzle exit)
4. Chamber pressure,  $p_c$  (jet stretcher ambient)
5. Test body static pressures,  $p_B$ , in one-inch increments from the model nose. The test body was rolled to obtain the circumferential pressure distribution.

These pressures were measured with strain-gage-type transducers. The transducers were periodically calibrated in the laboratory, and the data acquisition system (including the transducers) was resistance calibrated before and after each test period. The temperature recording system was millivolt calibrated before each test period.

### 3.2.3 Data Acquisition

All pressure and temperature data were recorded on a computer-controlled Digital Data Acquisition System (DDAS). All data obtained on the DDAS were recorded on magnetic tape in digital form at a scan rate of 20,000 channels/sec. Recorded data were obtained in both on-line and off-line modes of operation. The estimated accuracy of the pressure data is  $\pm 0.5$  percent. The accuracy of the temperature data is  $\pm 2.0^\circ\text{F}$ .

## 3.3 EXPERIMENTAL RESULTS

### 3.3.1 Design Configuration

The design configuration is for zero angle of attack as shown in Fig. 3. The mismatch angle between the jet stretcher and the computed interference-free flow field in this configuration is presented in Fig. 4 for both the measured (Table I) and the aerodynamic jet stretcher contours. The aerodynamic jet stretcher contour was obtained by correcting the measured contour for boundary layer growth computed by Tucker's method (Ref. 2). Ideally, the mismatch angle for the aerodynamic contour should be zero since this is the design configuration. The deviations from the ideal shown in Fig. 4 are due to fabrication errors but do not exceed the  $\pm 0.5$ -deg criterion for acceptable aerodynamic testing.

The major aerodynamic features of this configuration are shown in Fig. 5. The nozzle boundary layer was computed by Bartz method (Ref. 3) and the interference-free flow field by the method of Ref. 4. The Mach lines were estimated by the method presented in Appendix III and show that the jet stretcher influence begins at station 13.8 on the

test body. Flow over the upstream portion of the forebody can only be influenced by the nozzle flow.

Experimental static pressure distributions along the top ( $\theta = 0$  deg) and bottom ( $\theta = 180$  deg) of the test body are presented in Fig. 6. The nozzle influence extends to station 13.8, and the results show that no major disturbances were produced by the nozzle. The differences between the experimental data for the top and bottom of the test body are due to a slight change in angle of attack as the test body is rolled. The results also show that no major disturbances were produced by the jet stretcher.

These results verify the jet stretcher concept for zero angle of attack testing.

### 3.3.2 Test Body at 4-deg Angle of Attack

The optimum position of the test body is that which allows the bow shock wave to pass through the edge of the nozzle exit boundary layer at the nozzle exit plane (Fig. 5). This allows the jet stretcher to be located as close as possible to the nozzle exit in order to block undesirable disturbances from within the nozzle produced by a difference in pressure between the nozzle exit and the test cell.

For this test configuration, the test body was set near the optimum position by pitching the test body 4 deg about its nose from the zero angle-of-attack position as shown in Fig. 7. This was done for mechanical convenience since the optimum position would require translating the test body vertically by about 0.2 in. and horizontally by about 0.1 in. in order to correctly position the bow shock wave.

The optimum position of the jet stretcher was determined by computing the mismatch angle for various orientations of the jet stretcher. These results showed that the optimum position of the jet stretcher is obtained by pitching the jet stretcher about the nose of the test body through an angle of 1.5 deg from its design position at zero angle of attack. The region of jet stretcher influence on the test body is shown in Fig. 7. The mismatch angles ( $\beta$ ) for the top and bottom of the jet stretcher are presented in Fig. 8. The results show that the top of the jet stretcher is acceptably matched over the entire length that can influence the test body. However, the bottom of the jet stretcher requires porosity in the region from station 4.4 to 7.7 in., and, since the mismatch angle is negative in this region, in-bleed is required.

The circumferential distribution of the porosity area on the jet stretcher surface was estimated by assuming a trigonometric variation in mismatch angle between the top and bottom of the jet stretcher. The theoretical and experimental results presented in Ref. 5 show that this is a good assumption for this test body. The location of the porosity area on the jet stretcher and the porosity hole pattern are presented in Figs. 9a and b.

The amount of porosity required for complete cancellation of the disturbances is a function of the local mismatch angle ( $\beta$ ), the local pressure difference across the jet stretcher wall, and the corresponding characteristics of the porous wall. At the present time, it is not possible to theoretically predict the characteristic of a porous wall with

sufficient accuracy to obtain a realistic estimate of the required jet stretcher porosity. However, for the experimental apparatus used in this study, it was possible to independently control the jet stretcher ambient pressure and, thus, control the pressure difference across the porous wall (bleed flow). Therefore, the amount of porosity was not a critical factor and a uniform hole pattern having about 7-percent porosity (open area to closed area) was used (Fig. 9b). Experimental results were obtained for various jet stretcher ambient pressure levels, and the optimum value was determined from the measured pressure distribution on the test body.

The experimental static pressure distributions on the test model for roll angles ( $\theta$ ) of 0, 90, 120, 150, and 180 deg are presented in Figs. 10a, b, c, d and e, respectively. These experimental results with the jet stretcher are in good agreement with the corresponding results for interference-free flow. The influence of bleed flow through the porous region is shown in the pressure distribution on the windward side ( $\theta = 180$  deg) of the test body. For small bleed flows ( $p_c/p_N = 1.0$ ), an expansion wave disturbance occurs in the region requiring porosity as predicted by the theory. The optimum bleed flow occurs for a pressure ratio ( $p_c/p_N$ ) of about 1.4. Fortunately the pressure ratio for optimum bleed flow is less than the maximum pressure ratio allowable for this jet stretcher configuration. The maximum allowable chamber pressure ( $p_c$ ) is determined by the occurrence of disturbances from the nozzle produced by the feedback of the high chamber pressure ( $p_c$ ) through the subsonic portion of the nozzle boundary layer. The effect of such a disturbance on the model pressure coefficient is shown in Fig. 10a for a chamber pressure ratio ( $p_c/p_N$ ) of 1.857. An analysis of the pressure feedback in a turbulent boundary layer is presented in Ref. 6.

### 3.3.3 Test Body at 8-deg Angle of Attack

For this test configuration, the near optimum location of the test body was obtained by pitching the test body about station 5 (5.0 in. aft of the nose) through an angle of 8 deg from its position in the zero angle-of-attack test configuration.

It was not possible to acceptably match the jet stretcher inlet to the interference-free flow field. When the bottom of the jet stretcher was acceptably matched, the top of the jet stretcher was at too steep an angle. However, the quality of the inlet flow at the bottom of the jet stretcher is much more influential than at the top so that a near optimum jet stretcher position is obtained by acceptably matching the bottom inlet of the jet stretcher. This was done by the following movements of the jet stretcher from its design position at zero angle of attack. First, the jet stretcher was translated vertically until its centerline passed through the nose of the test body after it was set at an 8-deg angle of attack. Based on calculations to optimize the mismatch angle ( $\beta$ ), the jet stretcher was pitched about the nose of the test body through an angle of 3.5 deg. A sketch of the test configuration showing the major aerodynamic features is presented in Fig. 11. The mismatch angles for the top and bottom of the jet stretcher are presented in Fig. 12. The mismatch angle ( $\beta$ ) for the top of the jet stretcher varies from 1.2 to 1.6 deg over the length that can influence the flow over the test body. This angle exceeds the acceptable tolerance of  $\pm 0.5$  deg for aerodynamic testing and should produce undesirable compression disturbances. The bottom of the jet stretcher required porosity from station

3.7 to 7.7 in., which is essentially the same region as that for testing at a 4-deg angle of attack. Therefore, the porosity pattern was not changed.

Experimental pressure distributions on the test body are compared with theory and experiment for interference-free flow in Figs. 13a, b, c, d and e for corresponding roll angles ( $\theta$ ) of 0, 90, 120, 150, and 180 deg. These results show that there are no major disturbances produced by the jet stretcher, not even by the top of the jet stretcher which did not match the established criteria for aerodynamic testing. The bottom of the jet stretcher is the most critical, and the experimental results presented in Fig. 13e clearly show the expansion-type disturbance predicted by the theory. The porosity was located in the correct position to reduce this disturbance; however, the maximum chamber pressure ratio ( $p_c/p_N$ ) of 1.4 allowed by this configuration did not produce enough bleed flow to be effective. This indicates that the amount of porosity should be increased.

### 3.4 SIGNIFICANCE OF RESULTS

#### 3.4.1 Angle-of-Attack Limit Using an Axisymmetric Jet Stretcher

The angle-of-attack limit of this testing technique is determined by a definition of acceptable jet stretcher performance that is consistent with the test requirements. In this study, this criterion for aerodynamic testing was based on maintaining the static pressure distribution on the test body to within  $\pm 10$  percent of the interference-free flow pressure distribution. The experimental results for the axisymmetric jet stretcher system tested show that the angle-of-attack limit for aerodynamic testing is 4.75 deg. This was determined from the experimental results at 4- and 8-deg angle of attack by assuming that the strength of a disturbance from the jet stretcher varies linearly with angle of attack at the aft end of the test body on the leeward side. This station was selected because the theory shows it to be the point of maximum jet stretcher influence.

It should be noted that this angle of attack limit of 4.75 deg is for an axisymmetric jet stretcher and can be significantly increased by the use of a nonaxisymmetric jet stretcher, as is discussed in Section 3.4.3.

#### 3.4.2 Importance of Porosity

Both theory and experiment show that porosity is of secondary importance for this testing technique since the major disturbances are eliminated by properly positioning the jet stretcher. In this small scale experimental study, the amount of porosity was not a critical factor since it was possible to control the bleed flow by varying the jet stretcher ambient pressure with the ETF exhaust system. However, when testing in a full-scale test facility, the jet stretcher ambient pressure will be constant at a level determined by the exhaust diffuser performance unless some auxiliary pumping system is used. Consequently, the amount of porosity will be critical, and, at the present time, there are no satisfactory analytical techniques for solving this problem.

#### 3.4.3 Application to Airbreathing Propulsion Systems

The use of this technique for testing a vehicle with aft multiple inlets at moderate angles of attack is likely to be limited by geometric interference between the jet stretcher

and the lower engine inlets as shown in Fig. 14a. This interference problem can be eliminated by modifying the axisymmetric jet stretcher with wedge-shaped spacers which increase the exit area of the jet stretcher as shown in Fig. 14b. The optimum position of such a jet stretcher would be obtained by acceptably matching the bottom of the jet stretcher inlet in a position that also avoids geometric interference with the lower engine inlets on the test body. The spacers would then pitch the jet stretcher top to a more favorable matching condition since, as previously indicated for an axisymmetric jet stretcher, the top is at too steep an angle when the bottom is acceptably matched. Thus, the use of spacers not only eliminates geometric interference but also improves the matching of the top of the jet stretcher.

#### SECTION IV CONCLUSIONS

The results of a study of the feasibility of using a porous, axisymmetric jet stretcher for angle-of-attack testing of missiles having aft-located engine inlets are summarized as follows:

1. An axisymmetric, porous jet stretcher can be used for angle-of-attack testing. For an axisymmetric jet stretcher system similar to that studied, the maximum angle of attack for maintaining the pressure distribution to within  $\pm 10$  percent is 4.75 deg.
2. The analytical technique for evaluating the off-design performance of a jet stretcher has been experimentally verified for angles of attack up to 8 deg.
3. The major areas for improving this testing technique are:
  - a. Elimination of undesired disturbances from within the nozzle produced by the feedback of the jet stretcher ambient pressure through the subsonic portion of the nozzle boundary layer.
  - b. Optimization of porosity for the stretcher system.
  - c. Improvement in the angle-of-attack capability of this testing technique by modifying an axisymmetric jet stretcher with wedge-shaped spacers which increase the exit area of the jet stretcher.

## REFERENCES

1. German, R.C. "Simulation of Supersonic Flow over a Body of Revolution Using an Axisymmetric Jet Stretcher." AEDC-TR-70-166 (AD875834), October 1970.
2. Tucker, Maurice. "Approximate Turbulent Boundary Layer Development in Plane Compressible Flow along Thermally Insulated Surfaces with Application to Supersonic Tunnel-Contour Corrections." NACA-TN-2045, March 1950.
3. Weinagold, H. D. "The ICRPG Turbulent Boundary Layer Reference Program." Pratt and Whitney Aircraft, July 1968.
4. General Applied Sciences Laboratory. "The Addition of Secondary Shock Capability and Modification to the GASL Three Dimensional Characteristics Program." GASL Report No. 653 (AD666742), August 1967.
5. Smith, F. B., Bauer, R. C., and Barebo, R. L. "The Jet Stretcher as an Aerodynamic/Propulsion Testing Tool." AIAA Propulsion Joint Specialist Conference, Colorado Springs, Colorado, June 9-13, 1969.
6. Bauer, R. C., Matkins, E. H., and Barebo, R. L. "A Theoretical and Experimental Study of a Jet Stretcher Diffuser System." AEDC-TR-72-26 (AD738646), March 1972.

- APPENDIXES**
- I. ILLUSTRATIONS**
  - II. TABLE**
  - III. APPROXIMATE MACH LINE ANALYSIS**

**Preceding page blank**

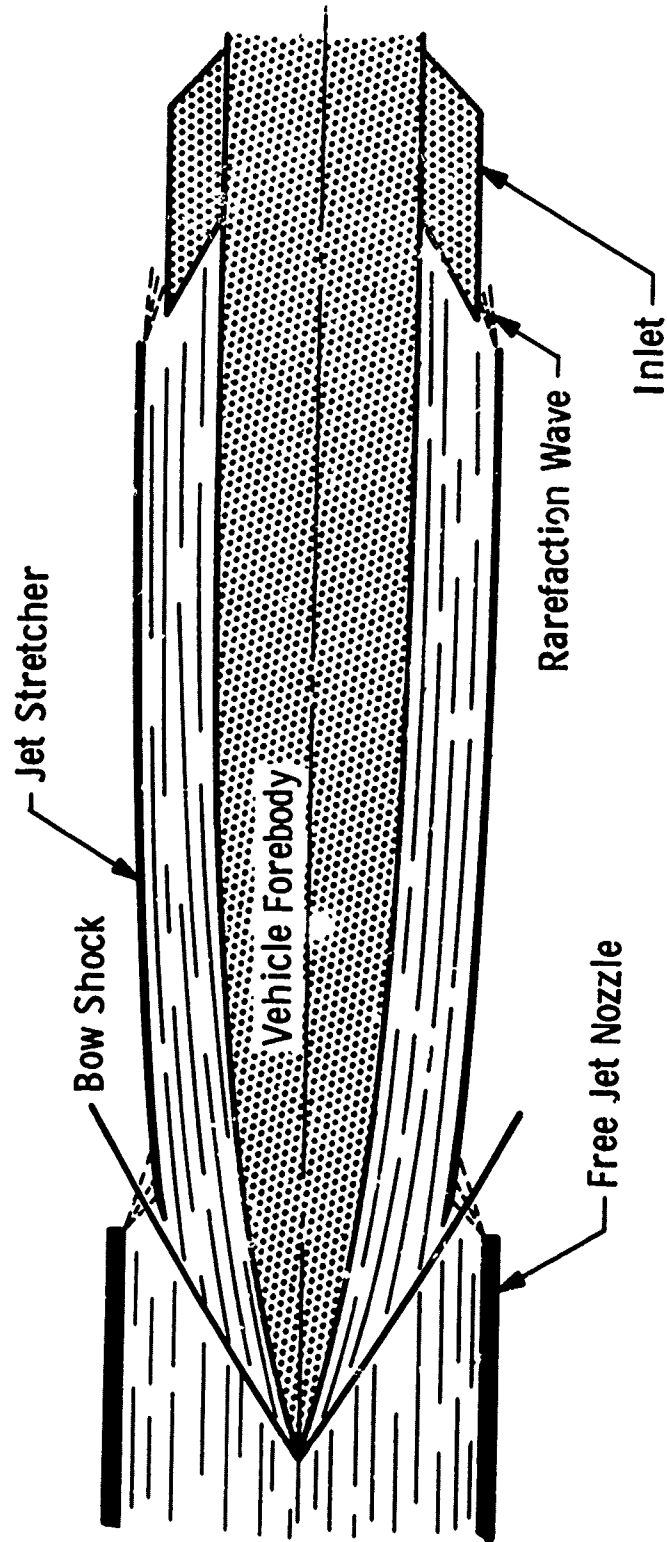


Fig. 1 Jet Stretcher Arrangement with Test Vehicle at Zero Angle of Attack

Preceding page blank

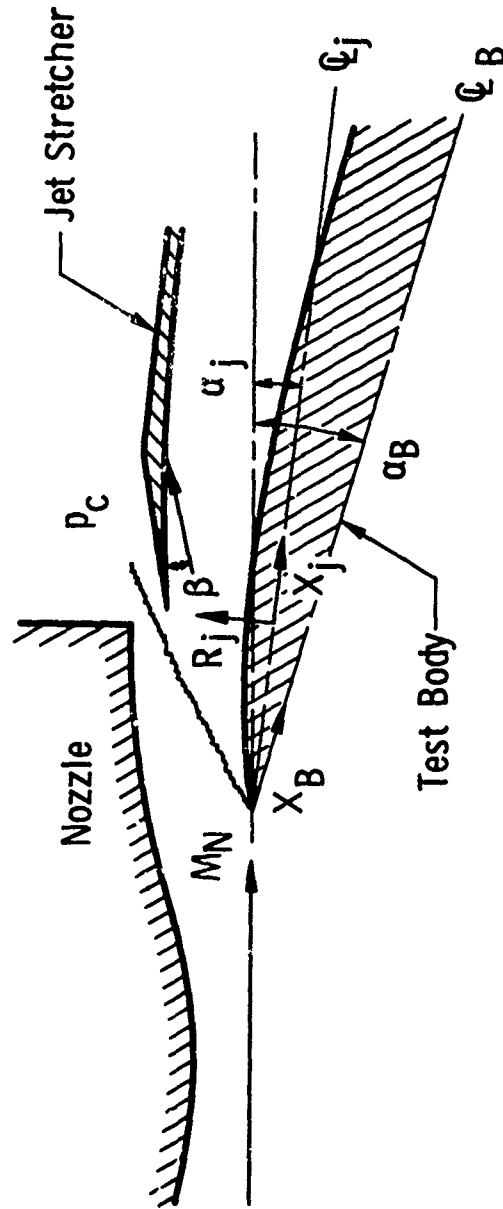


Fig. 2 Sketch Showing Jet Stretcher Mismatch Angle  $\beta$

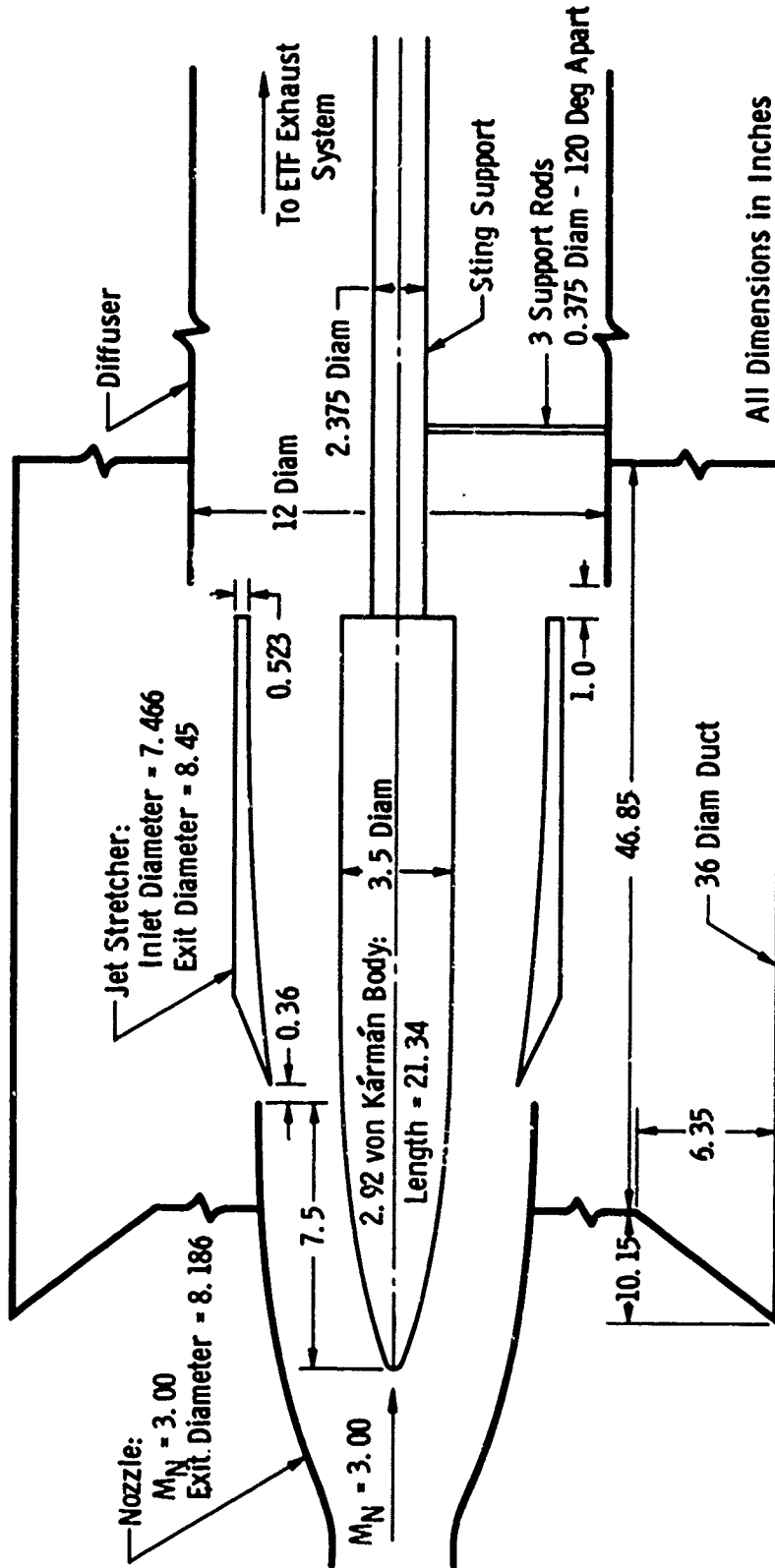


Fig. 3 Experimental Jet Stretcher-Diffuser System

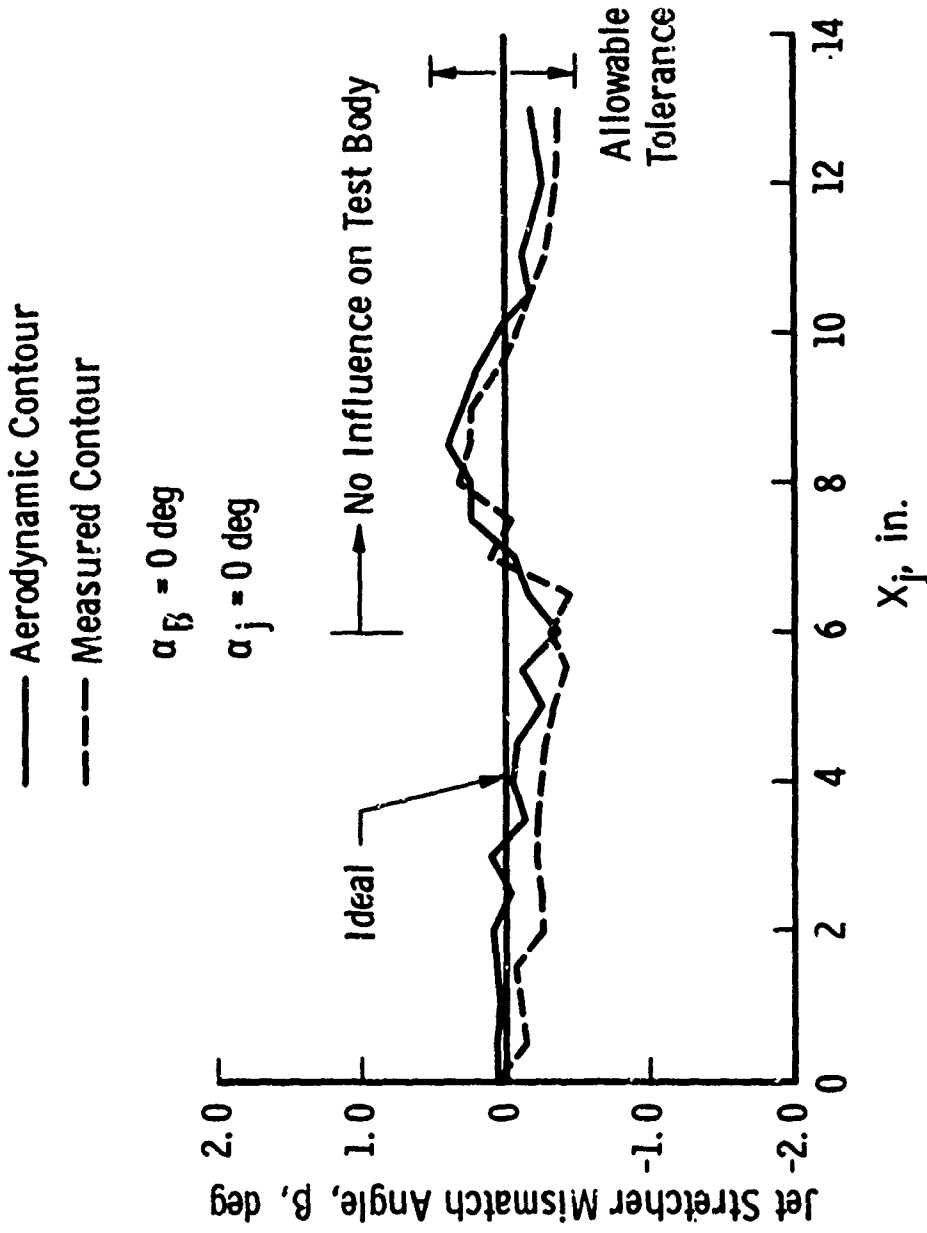


Fig. 4 Jet Stretcher Mismatch Angle for Design Configuration

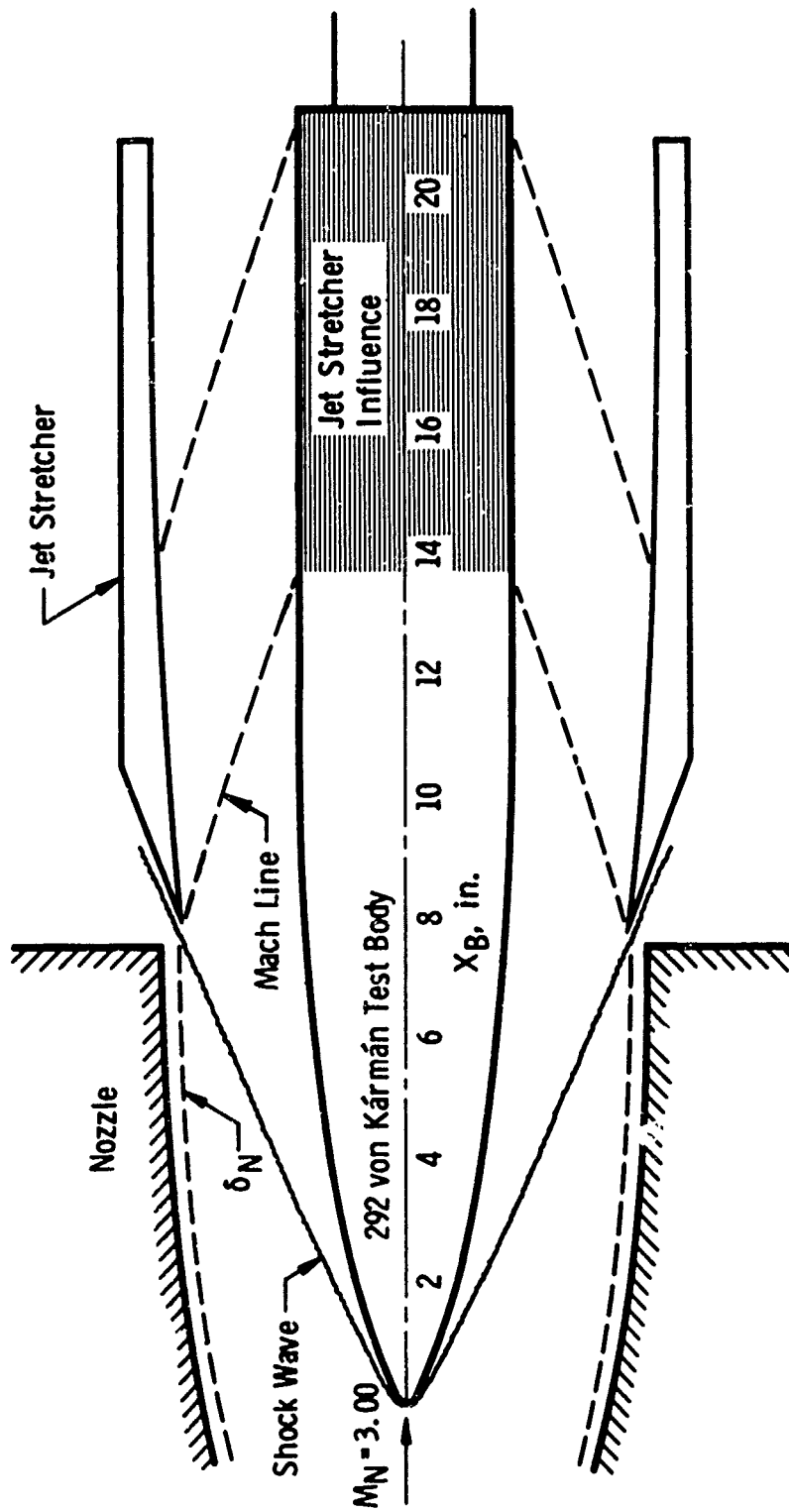


Fig. 5 Test Configuration with Test Body and Jet Stretcher at Zero Angle of Attack

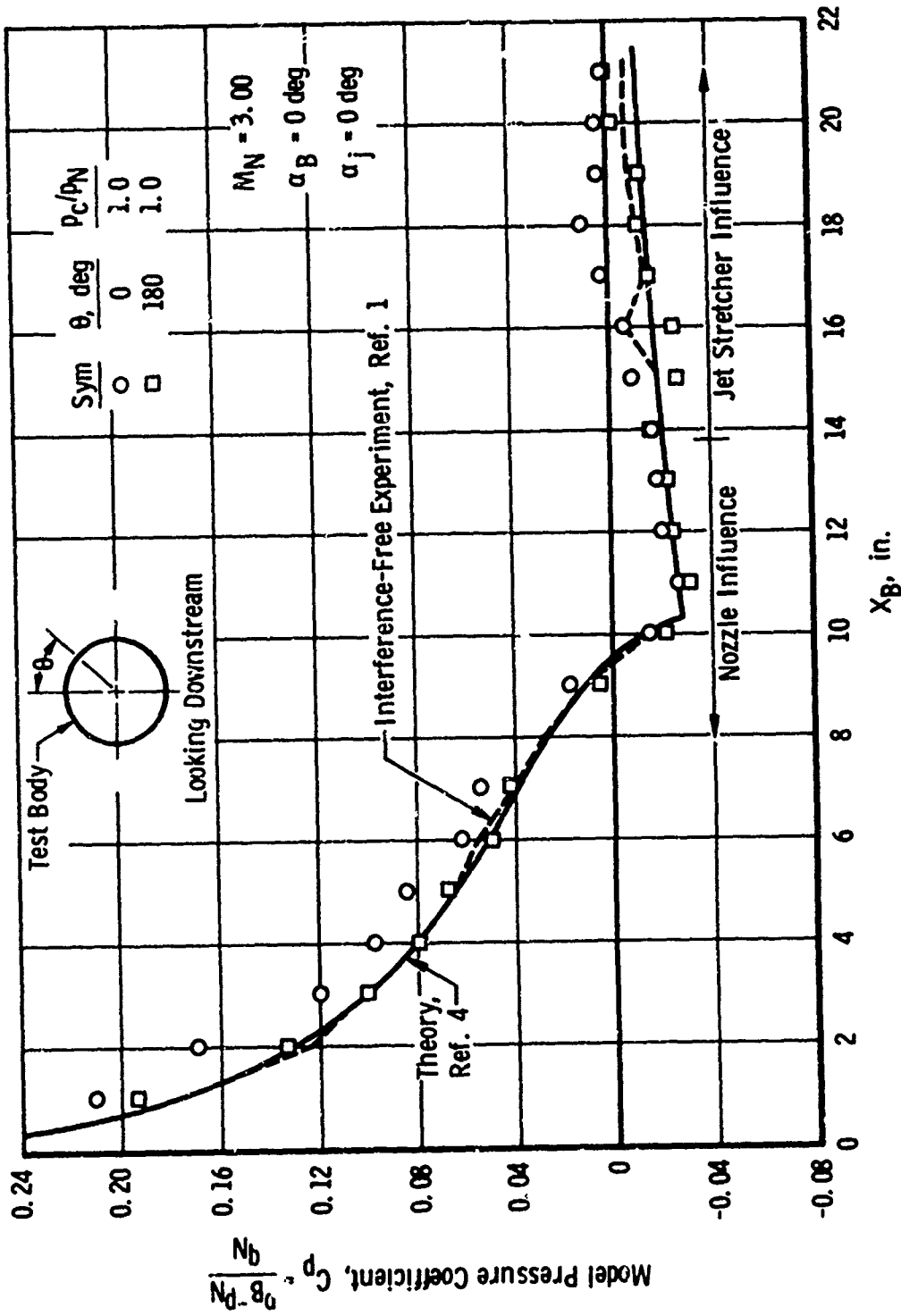


Fig. 6 Test Body Pressure Distribution for Zero Angle of Attack

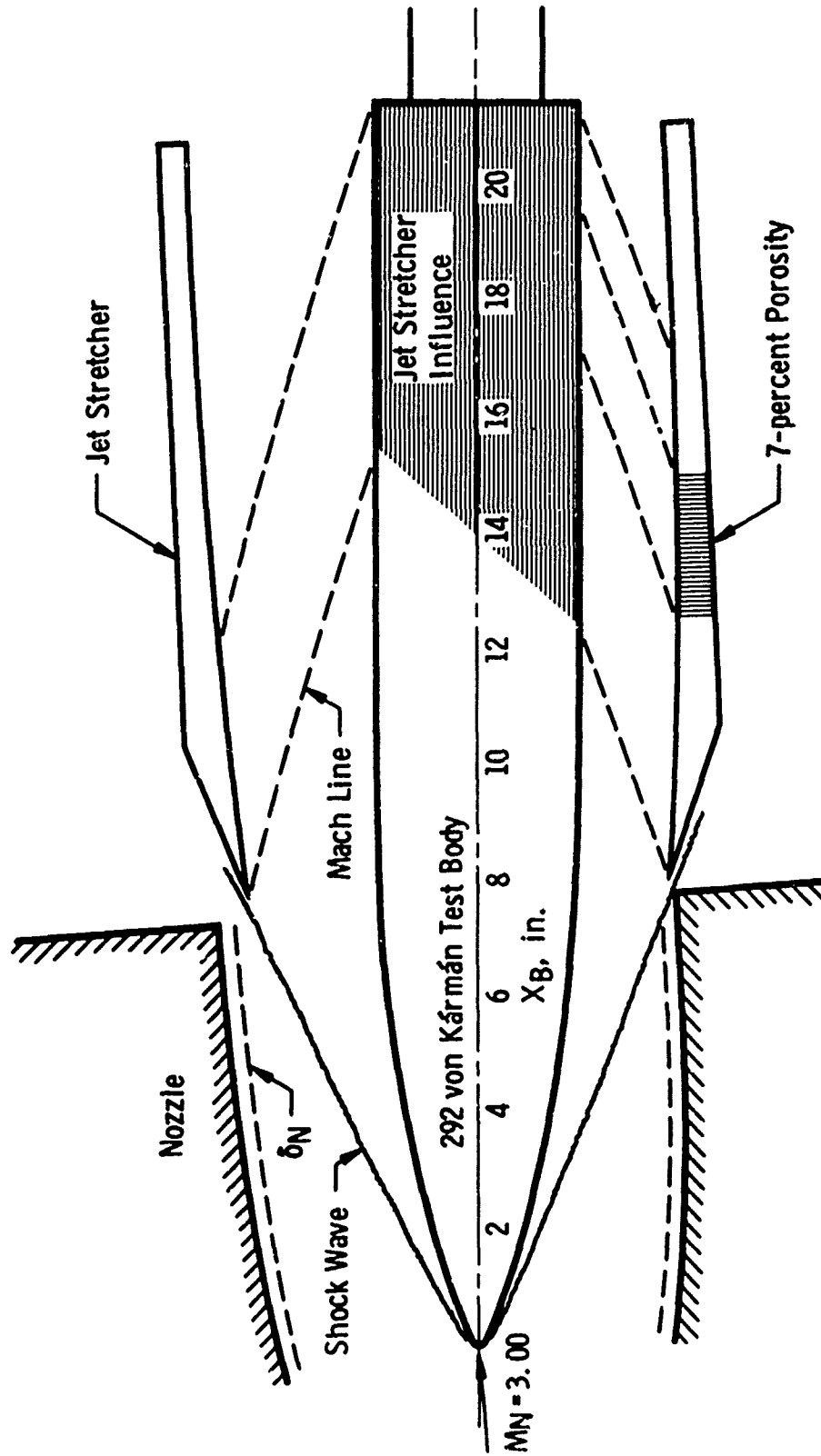


Fig. 7 Test Configuration with Test Body at 4-deg and Jet Stretcher at 1.5-deg Angles of Attack

Note: Calculation for Aerodynamic Contour With:

$$\alpha_B = 4 \text{ deg}$$

$$\alpha_j = 1.5 \text{ deg}$$

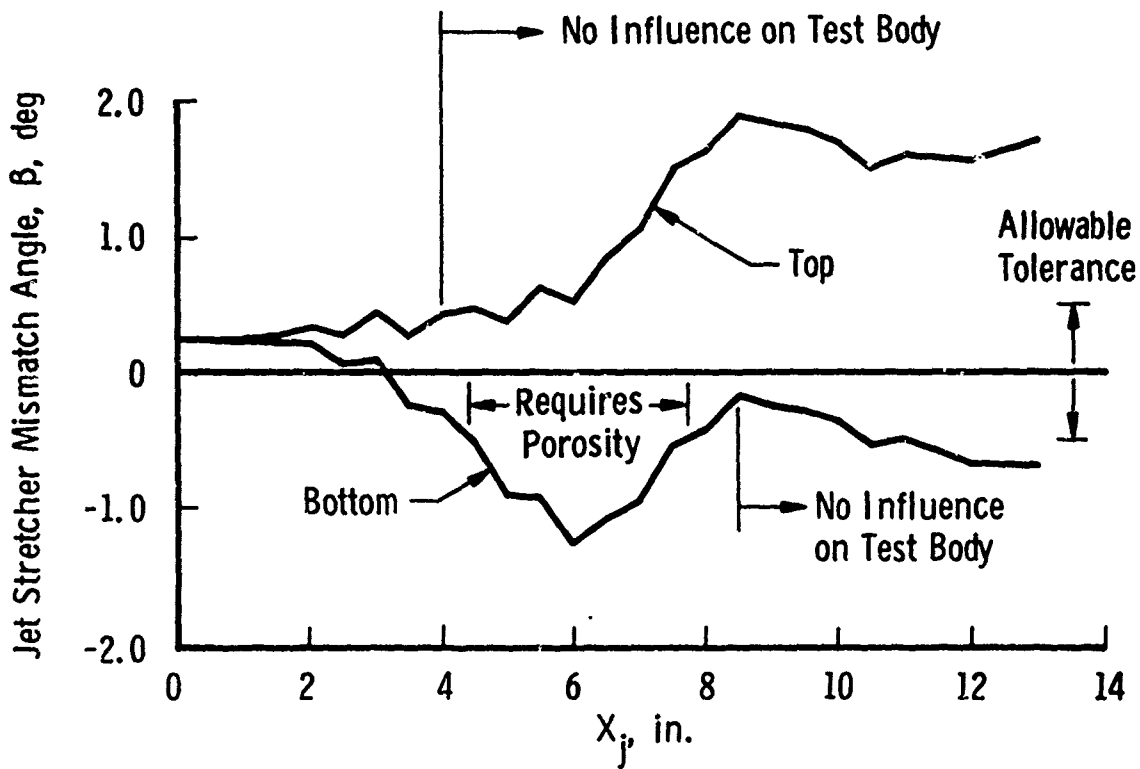
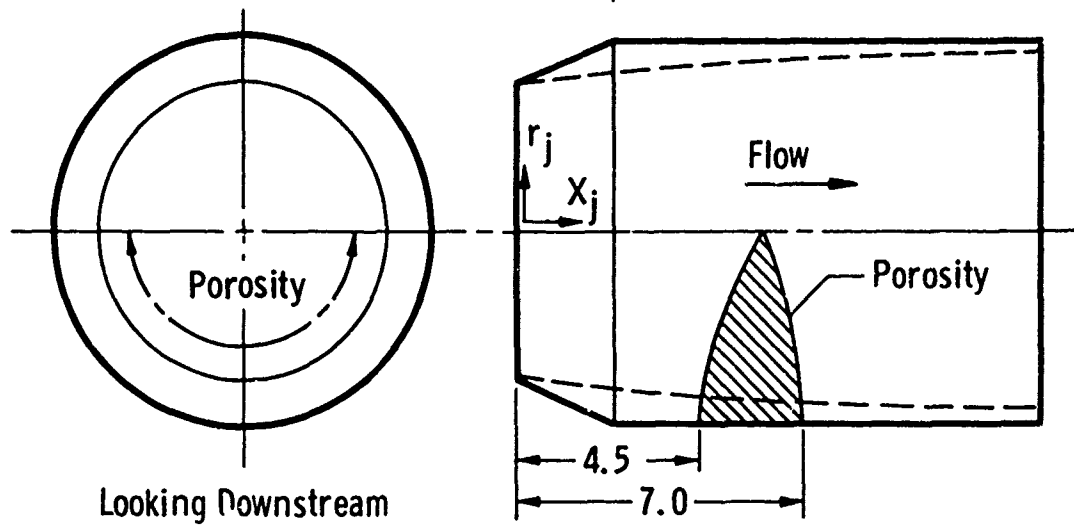
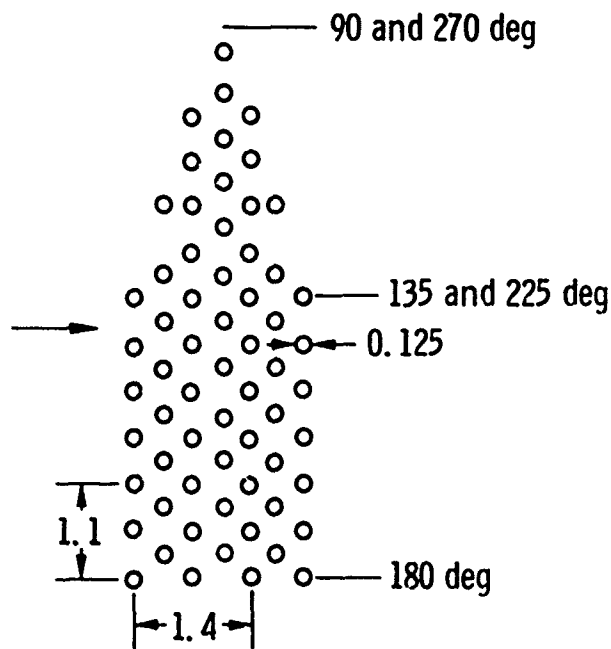


Fig. 8 Jet Stretcher Mismatch Angle with Test Body at 4-deg and Jet Stretcher at 1.5-deg Angles of Attack

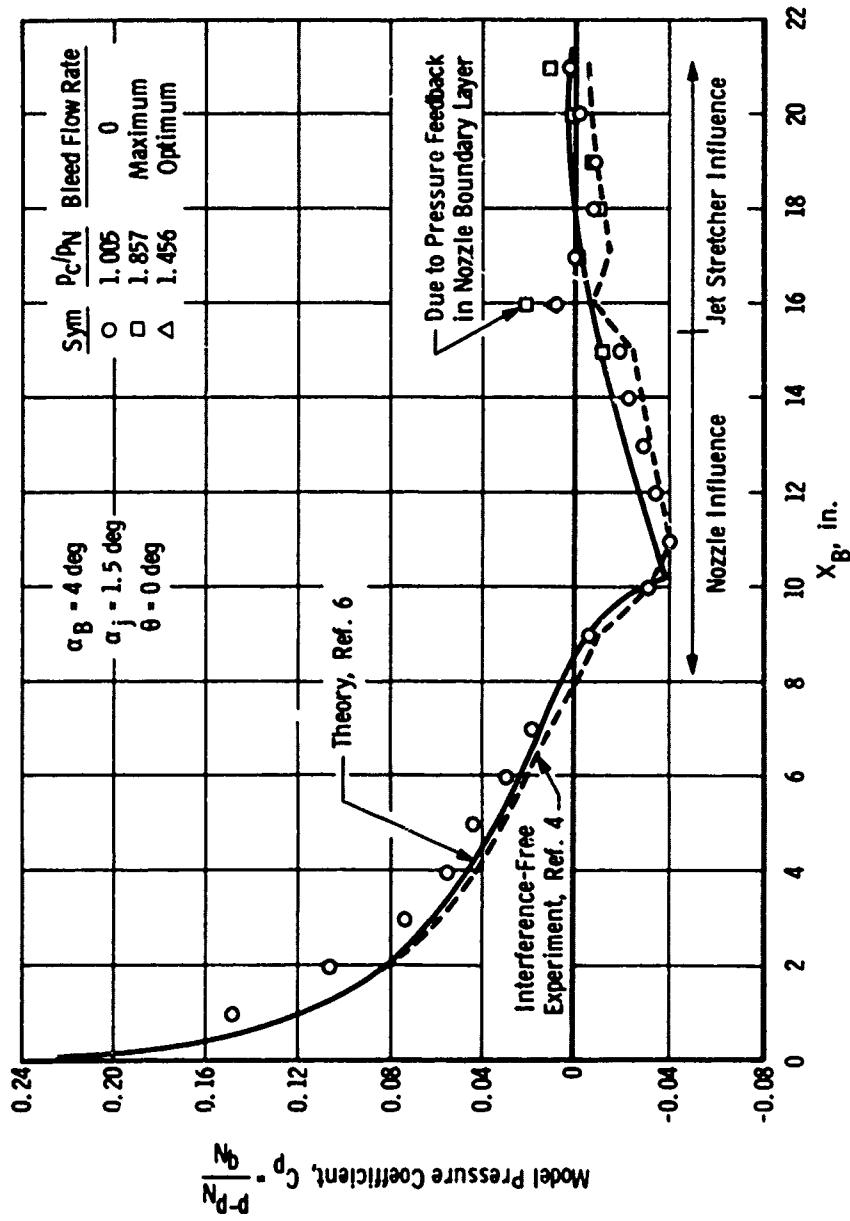


Looking Downstream

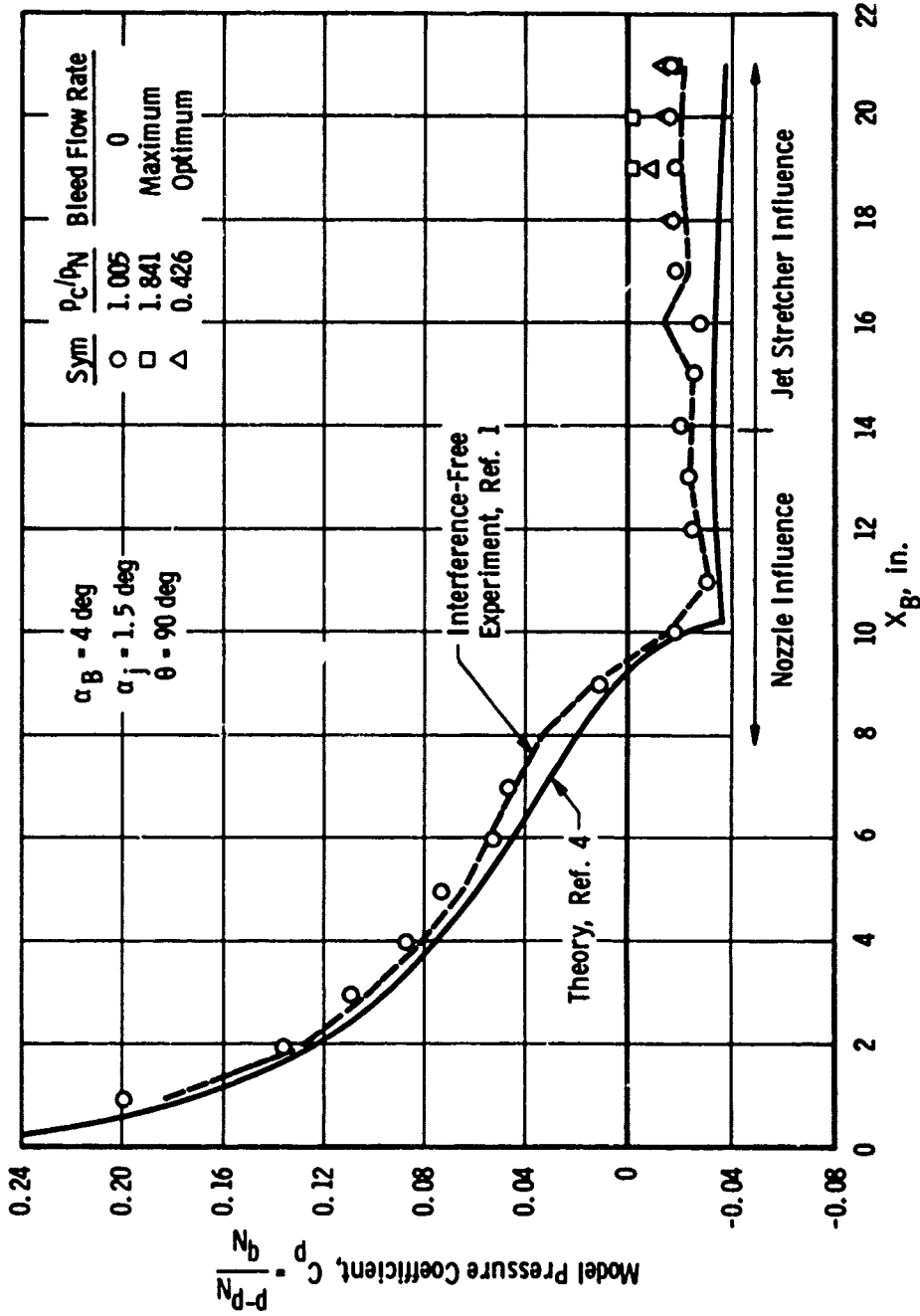
a. Location of Porosity



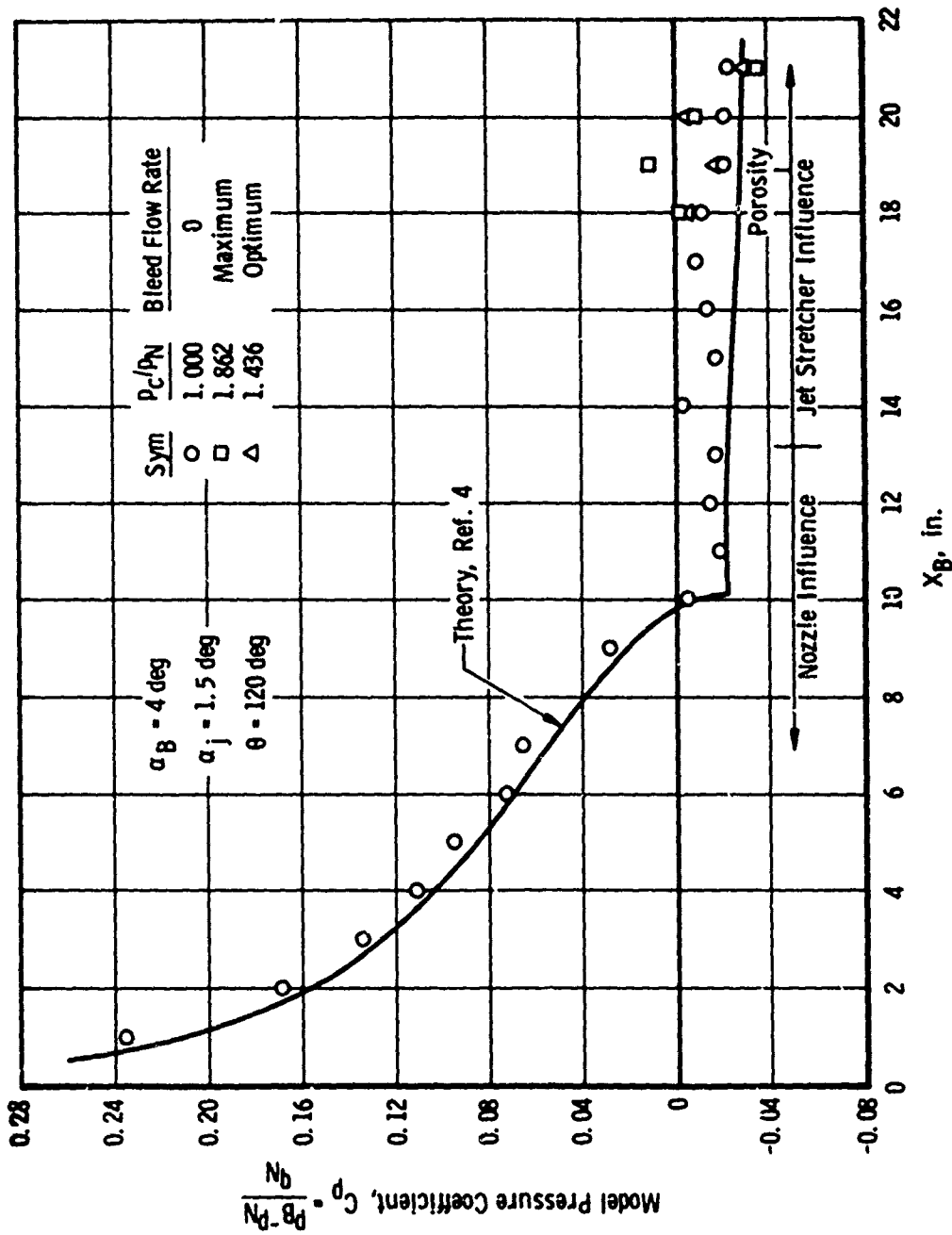
b. Porosity Hole Pattern  
Fig. 9 Jet Stretcher Porosity



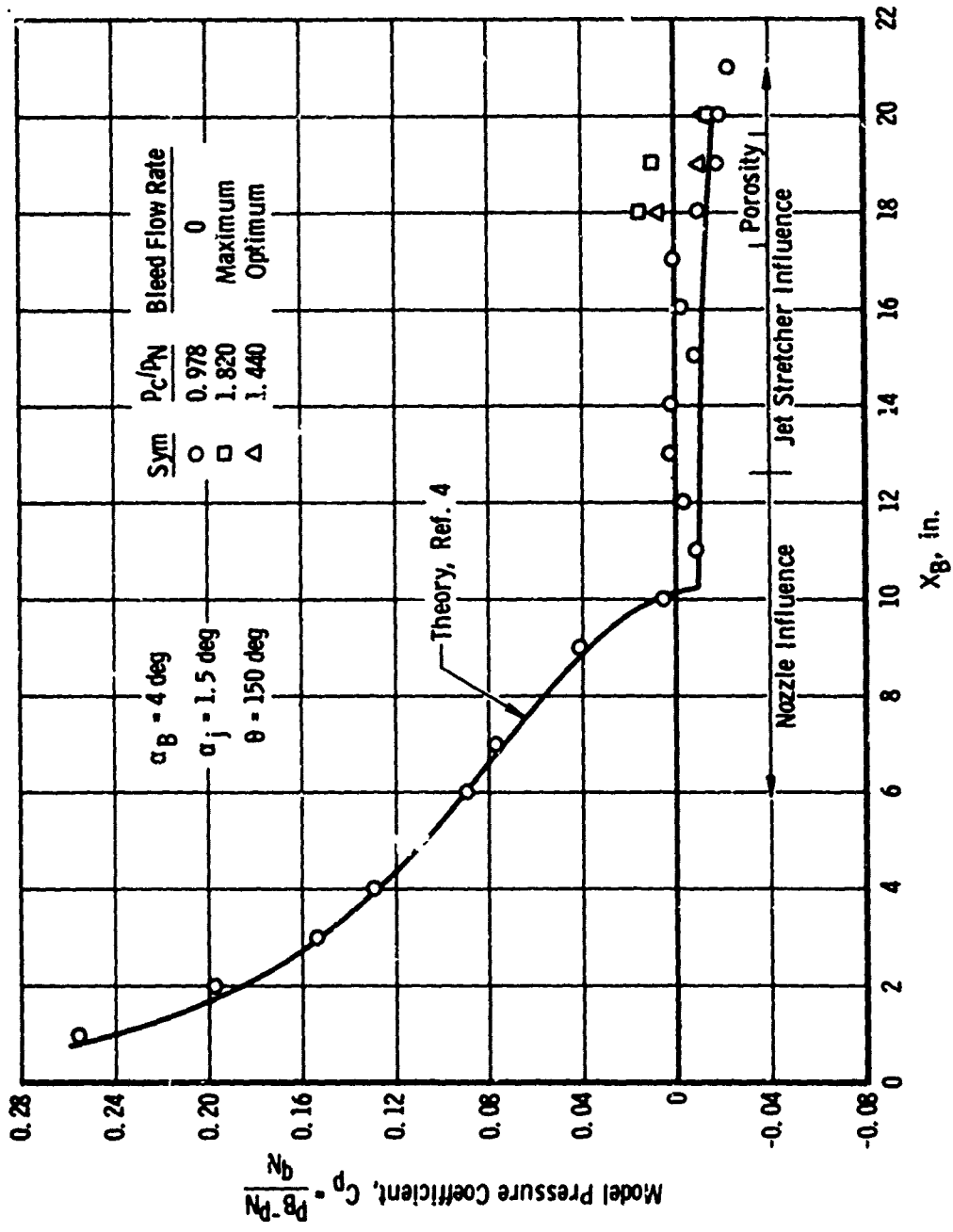
a.  $\theta = 0 \text{ deg}$  (Leeward Side)  
 Fig. 10 Test Body Pressure Distribution for 4-deg Angle of Attack



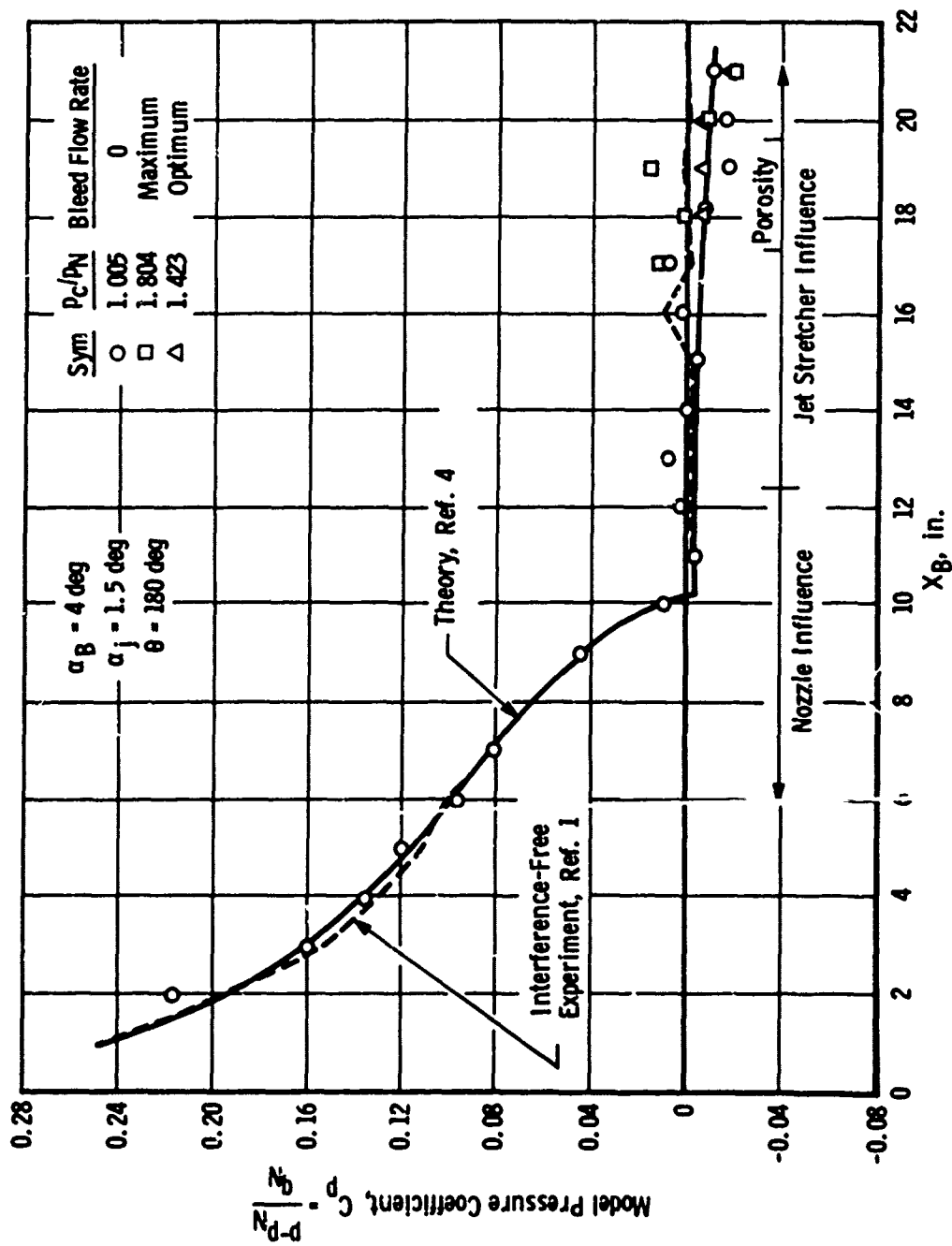
b.  $\theta = 90 \text{ deg}$   
 Fig. 10 Continued



c.  $\theta = 120 \text{ deg}$   
 Fig. 10 Continued



d.  $\theta = 150 \text{ deg}$   
 Fig. 10 Continued



e.  $\theta = 150$  deg (Windward Side)  
Fig. 10 Concluded

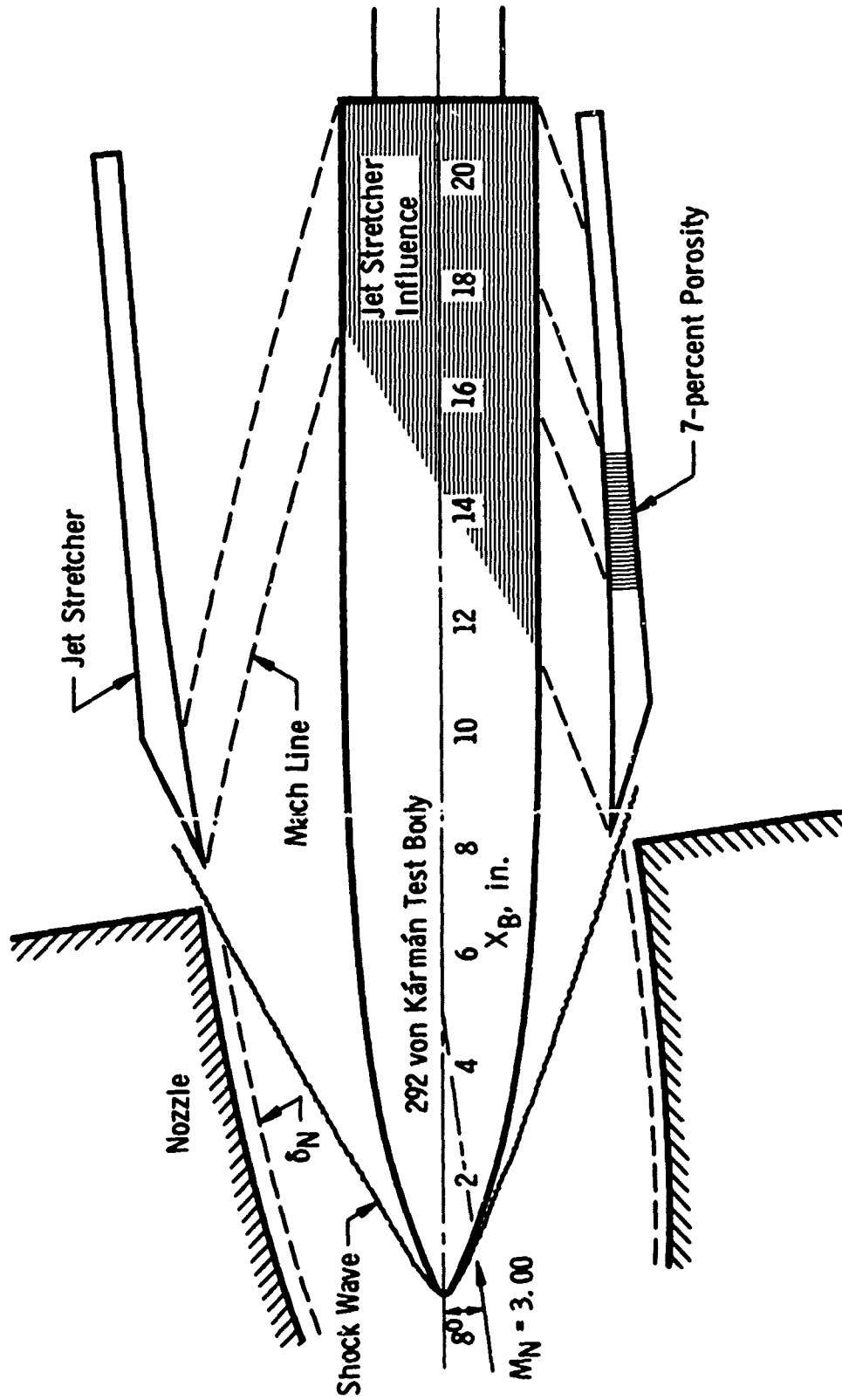


Fig. 11 Test Configuration with Test Body at 8-deg and Jet Stretcher at 3.5-deg Angles of Attack

Note: Calculation for Aerodynamic Contour With:  
 $\alpha_B = 8 \text{ deg}$   
 $\alpha_j = 3.5 \text{ deg}$

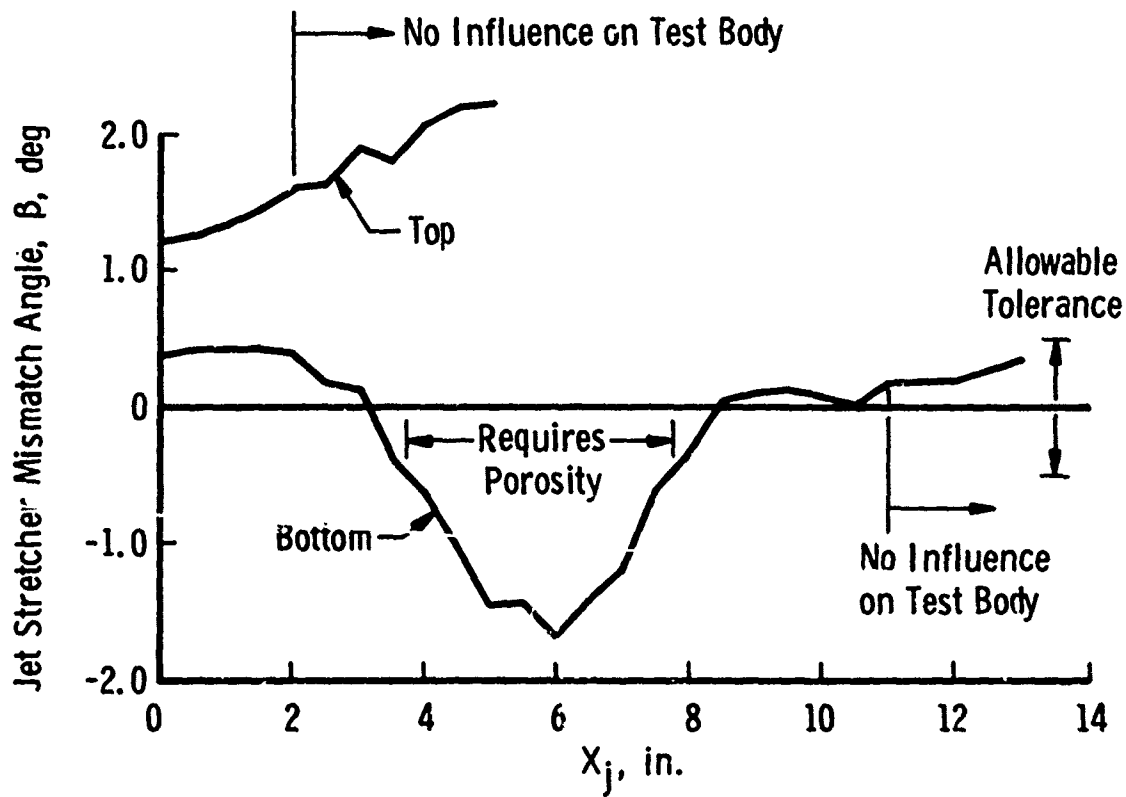
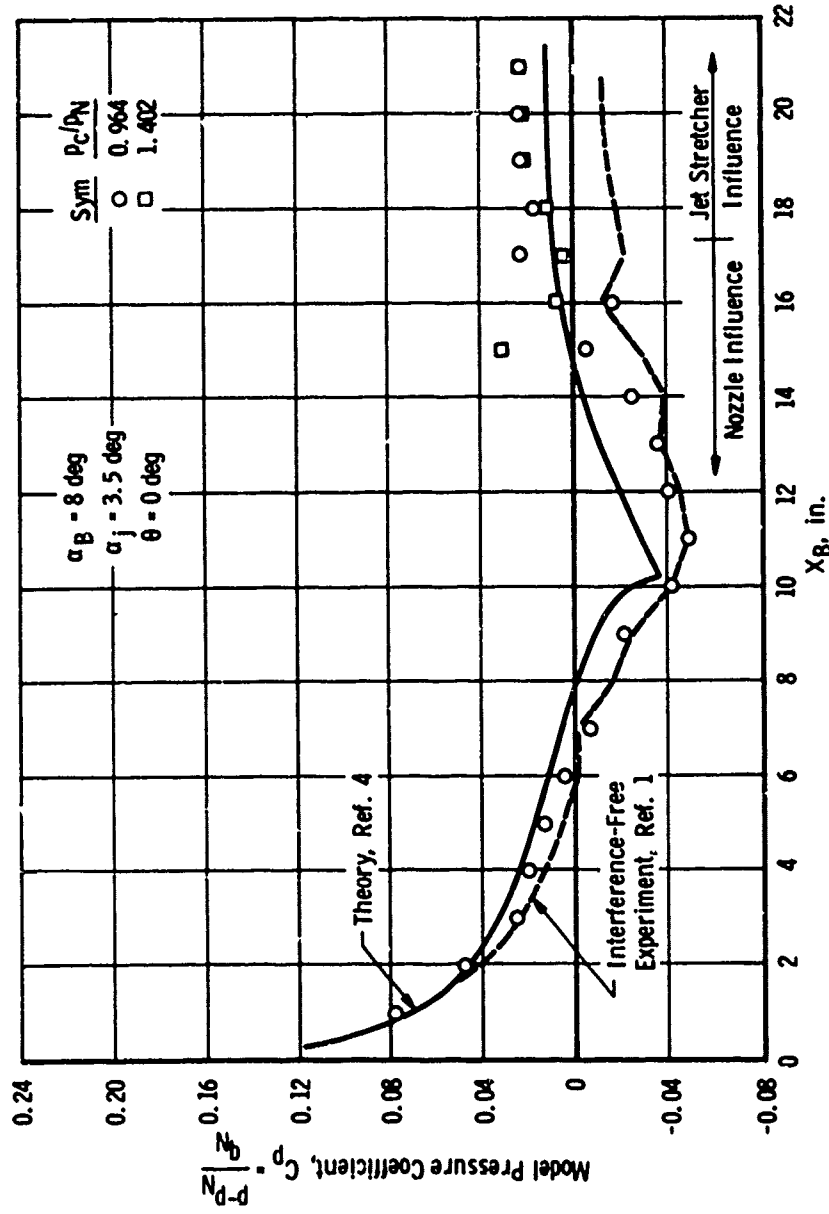
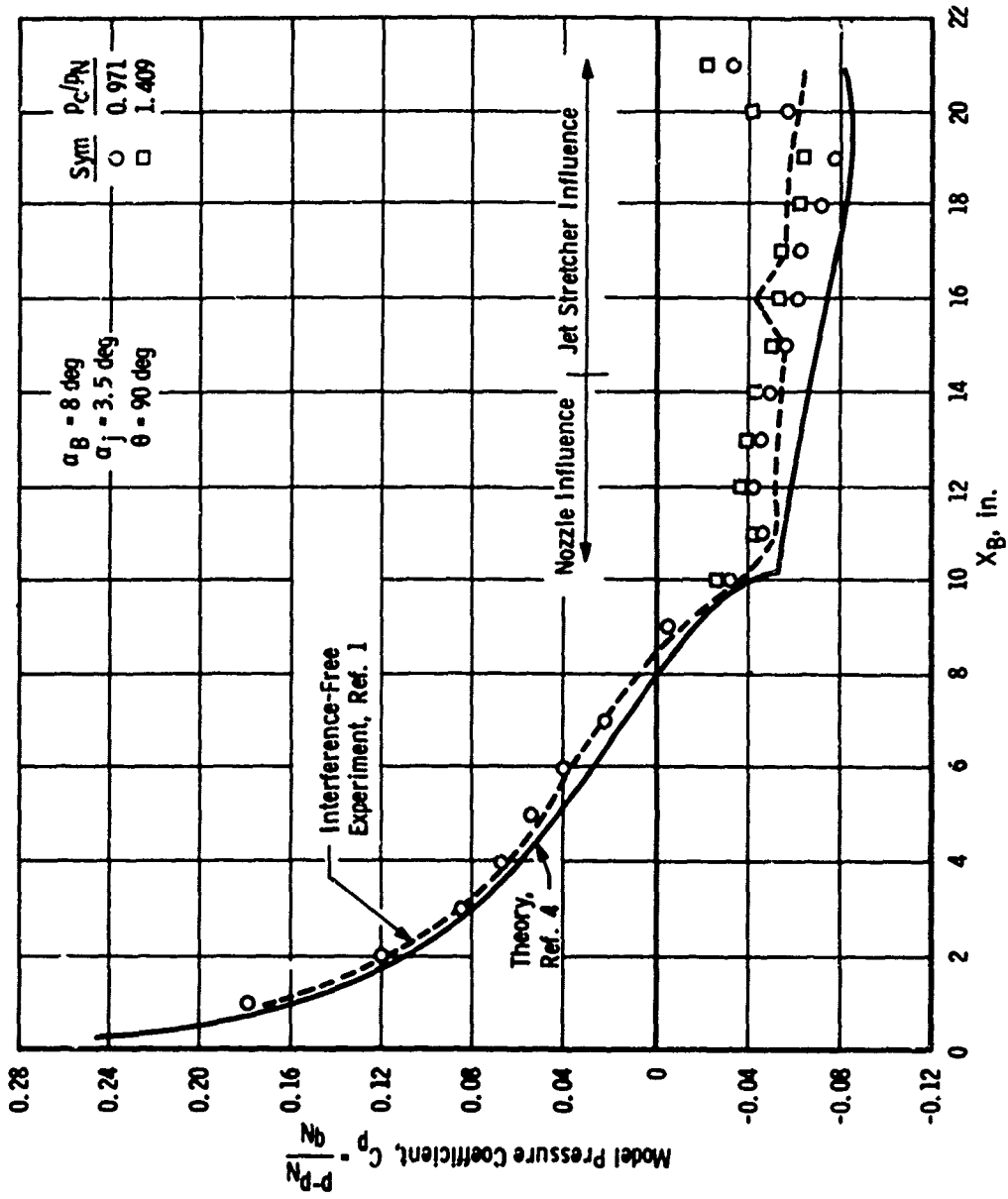


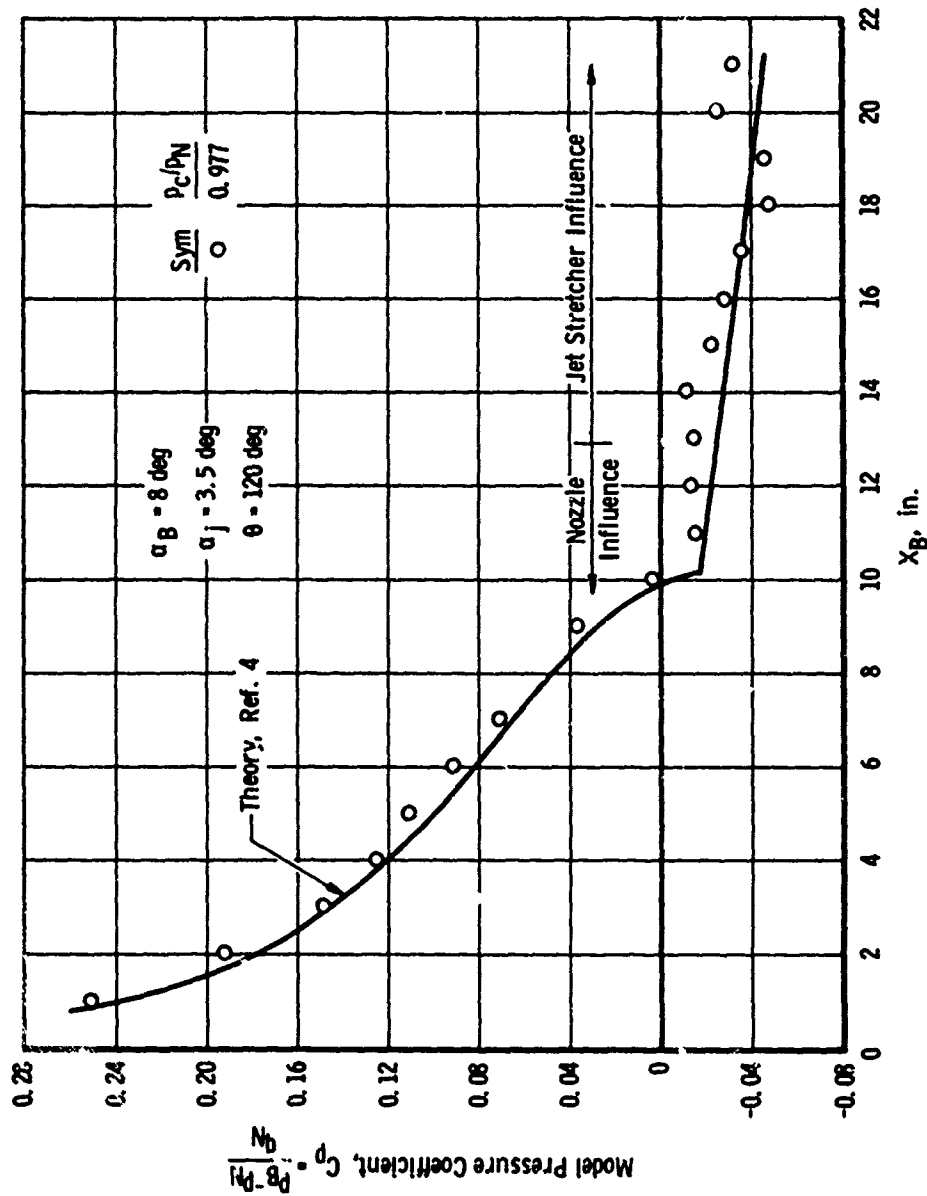
Fig. 12 Jet Stretcher Mismatch Angle with Test Body at 8-deg and Jet Stretcher at 3.5-deg Angles of Attack



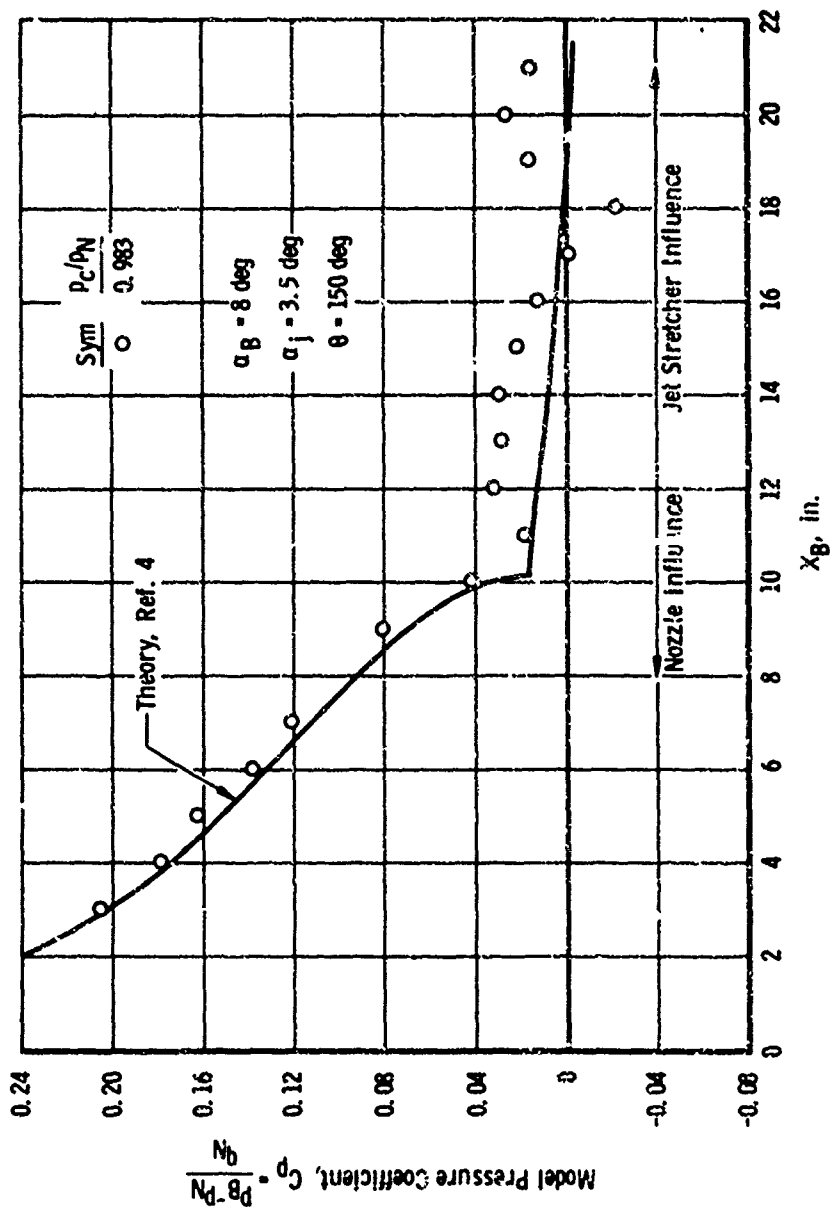
a.  $\theta = 0$  deg (Leeward Side)  
 Fig. 13 Test Body Pressure Distribution for 8-deg Angle of Attack



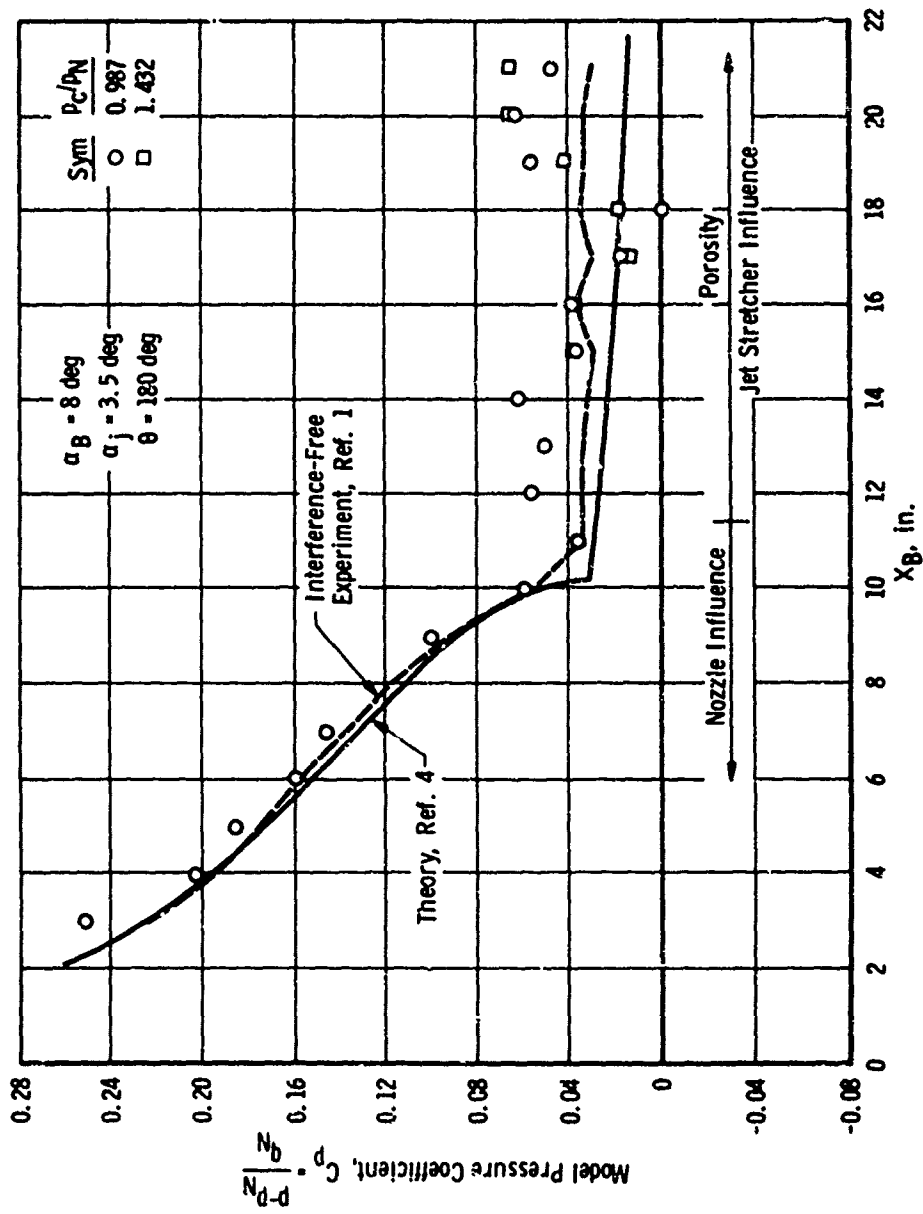
b.  $\theta = 90 \text{ deg}$   
 Fig. 13 Continued



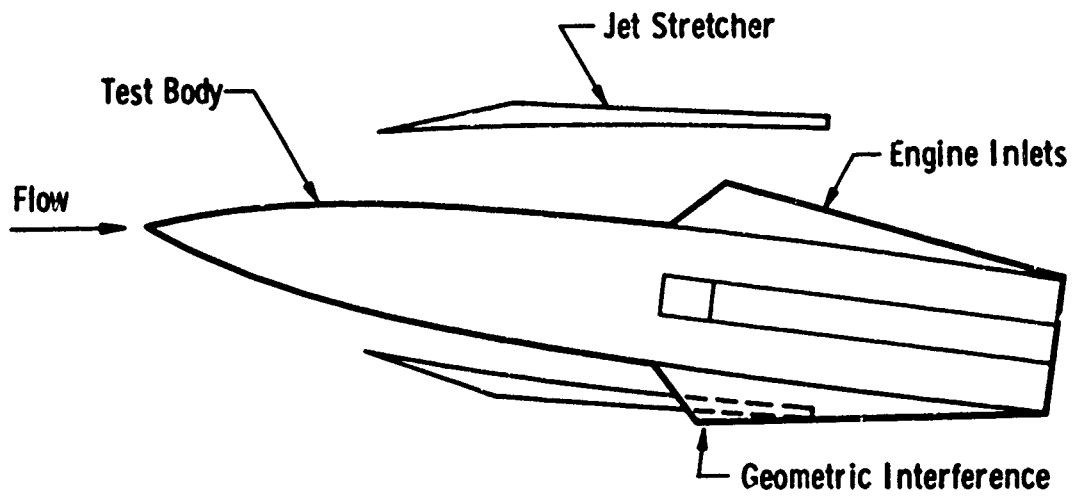
c.  $\theta = 120 \text{ deg}$   
 Fig. 13 Continued



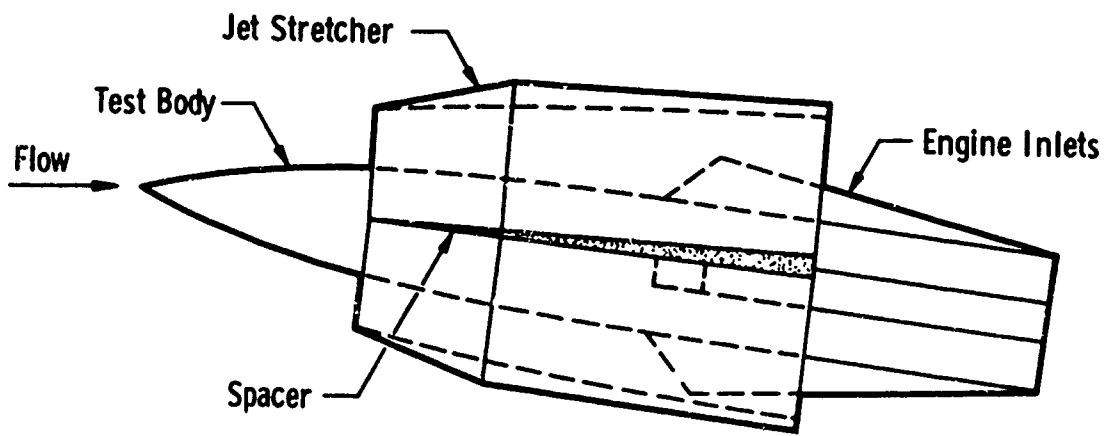
d.  $\theta = 150 \text{ deg}$   
Fig. 13 Continued



e.  $\theta = 180 \text{ deg}$  (Windward Side)  
 Fig. 13 Concluded



a. Axisymmetric Jet Stretcher in Optimum Position



b. Jet Stretcher with Spacers in Optimum Position  
Fig. 14 Application of Jet Stretcher with Spacers

TABLE I  
MEASURED JET STRETCHER COORDINATES

<u>X<sub>j</sub>, in.</u>	<u>R<sub>j</sub>, in.</u>	<u>ε<sub>j</sub>, deg</u>
0	3.733	5.040
0.5	3.777	5.040
1.0	3.821	4.812
1.5	3.863	4.580
2.0	3.903	4.580
2.5	3.942	4.355
3.0	3.978	4.125
3.5	4.014	3.898
4.0	4.047	3.668
4.5	4.078	3.440
5.0	4.108	3.210
5.5	4.134	2.980
6.0	4.159	2.521
6.5	4.179	2.292
7.0	4.195	1.375
7.5	4.205	1.146
8.0	4.212	0.459
8.5	4.215	0.229
9.0	4.217	0.229
9.5	4.218	0.115
10.0	4.219	0.115
10.5	4.221	0.229
11.0	4.222	0.115
12.0	4.225	0.172
13.0	4.226	0.057

### APPENDIX III APPROXIMATE MACH LINE ANALYSIS

The evaluation of jet stretcher performance is greatly facilitated by knowing the region on the test body where the flow is influenced by the jet stretcher. In order to save computer time, an approximate Mach line analysis was developed based on the following assumptions:

1. The shape of the Mach line is a circular arc.
2. The flow field along the Mach line is at a constant Mach number equal to the Mach number at the originating point of the Mach line. Only the flow angle varies along the Mach line.
3. The Mach line terminates on the cylindrical portion of the test body.

A sketch of an approximate Mach line is presented in Fig. III-1. The basic equation for the Mach line is

$$(X_B - n)^2 + (R_B - m)^2 = r^2 \quad \text{(III-1)}$$

The unknown quantities are  $n$ ,  $m$ ,  $r$ , and  $X_{B_i}$ . The known quantities are  $X_{B_1}$ ,  $R_{B_1}$ ,  $\epsilon$ ,  $\mu$ , and  $R_{BS}$ . Applying the boundary conditions illustrated in Fig. III-1 to Eq. (III-1) yields the following equation for the impingement distance ( $X_{B_i}$ ):

$$X_{B_i} = X_{B_1} + \left[ \frac{\sin \mu - \sin (\mu - \epsilon)}{\cos \mu - \cos (\mu - \epsilon)} \right] (R_{BS} - R_{B_1}) \quad \text{(III-2)}$$

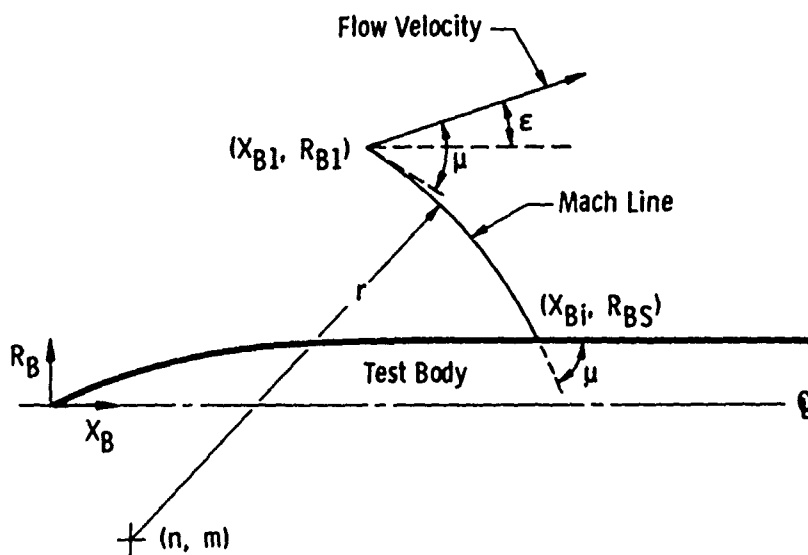


Fig. III-1 Sketch of Approximate Mach Line